

Muscle Mechanics Modeling

A Major Qualifying Project Report

Submitted to The Faculty

of

Worcester Polytechnic Institute

In partial fulfillment of the requirements for the

Degree of Bachelor of Science

by

Alina Orlovskaya

March, 2015

Approved:

Professor Sarah Olson

Abstract

This report focuses on investigating the data related to the human walk cycle with various perturbations. The biomechanics of muscle movement is discussed in the introduction. Then various muscle models, such as the Hill's muscle model, and spring model with a viscous contractile element are examined. This relates to the range of motion (ROM) of joints in relation to the force, angle and torque. Then human gait is introduced as the normal walk cycle and all the phases and sub-phases of the gait cycle are discussed. The data is given from subjects walking across force plate and the movement is measured with a goniometer. The bulk of the report compares data sets using statistical and analytical methods. In the gait data of 10 subjects, the ankle angle, center of pressure, and ground reaction force is compared between 2° and 5° perturbations, with perturbations occurring at 3 different timepoints in the gait. A perturbation is a deviation from the normal state of path caused by an outside influence of the tilt of the platform. Two and 5° is the angle of the tilt of the force plate. It examines the reaction of the ankle with respect to the change in the force plate via the perturbations that occurred at different time points. Minimums, maximums, correlation coefficient, slope and two different statistical tests were conducted. All the calculations were completed in *MATLAB* to understand patient variation and the influence of a perturbation on gait.

Executive Summary

This report investigates the data related to the human walk cycle with different perturbations that occur at three timepoints. The biomechanics of muscle movement is discussed in the introduction. It goes over the biology of the musculoskeletal system and the mechanics of muscle movement. Then there are various muscle models, such as the Hill's muscle model, which describes the relationship between forces in the muscles. The spring model with a viscous contractile element explains the muscle contraction using the parallel elements, series elements, and contractile elements. It continues with a description of how stiffness is measured, including regular and rotational stiffness. Then, the data is introduced with how the data was collected. Then human gait is described in detail as the normal walk cycle and all the phases and sub-phases of the gait cycle. The stance phase has five sub-phases and swing phase has 3 sub-phases. The data is given from subjects walking across force plate and the movement is measured with a goniometer. The ankle angle, center of pressure, and a ground reaction force is recorded. Each parameter is defined in terms of gait. The graphs of the data are presented with an initial analysis.

The bulk of the report compares data sets using statistical and analytical methods. In the gait data of 10 subjects, the ankle angle, center of pressure, and ground reaction force is compared between 2° and 5° perturbations, with perturbations occurring at 3 different timepoints in the gait, which is 100 ms, 225 ms and 350 ms. First the minimums and maximums are calculated and compared across the different perturbations. Then, the correlation coefficients are identified, along with a description of measurements. Then the t-test and Passing-Bablok analysis follow. After checking, the data fails to have a normal distribution, which results in no definite conclusions from the test. The data then undergoes ankle angle maximums analysis, which gives vast insight into the actions of the perturbations on the data. It examines the reaction of the ankle angle with respect to the change in the force plate by the perturbations that occurred at different time points. Several subject's data was displayed and discussed. The center of pressure analysis was next, which showed the perturbations as oscillations. These oscillations are fitted to a sine curve, and compared between the different perturbed data. The least squares analysis was conducted and presented. The ankle angle data were fit to the curve for each perturbation. The conclusion included the similar trend of the effect of the perturbations. With any perturbation, the curves of the stance phase followed a distinct pattern. There were three segments that showed the three main subphases of the stance. Then, the data with the perturbations that occurred earlier in the stance phase were more distant from the nominal data and the data perturbations that occurred further in the stance phase were able to return closer to the nominal data. This type of study can help develop better prosthetics or create better shoe designs by accounting for the way the foot reacts to random, uneven ground.

Acknowledgements

I would like to thank Professor Sarah Olson for advising my project and giving me guidance. Thank you for providing insight and all the necessary resources on this project. Without her, it would not be a successful multifaceted study. There was good assistance and support along the way.

I would like to thank the WPI librarian, Laura Hanlan, for helping me find background research and the data depository websites.

In addition, I want to thank Professor Karen Troy in the Biomedical department for meeting with me to explain some of the details of COP.

Overall, I would like to thank Worcester Polytechnic Institute for giving me the opportunity to do this project.

Contents

1	Background	7
1.1	Biology of Musculoskeletal System	7
1.2	The Mechanics of Muscle Movement	9
1.3	Hill's Model	11
1.4	Measuring Stiffness	14
2	Data Introduction	15
2.1	The Origin of the Data	15
2.2	Locomotion and Gait	17
2.3	Parameters	22
2.4	Data	24
3	Analysis and Results	30
3.1	Minimums and Maximums	30
3.2	Correlation Coefficient Analysis	31
3.3	T-Test Analysis	34
3.4	Passing-Bablok Regression	36
3.5	Ankle Angle Maximums Analysis	38
3.6	COP Analysis	44
3.7	COP Sine Fitting	48
3.8	Least Squares Analysis	49
4	Conclusion	54
4.1	Conclusion	54
4.2	Suggestions for Changes	55
A	MATLAB Code	56

List of Figures

1.1	Back Skeletal Muscles.	7
1.2	Front Skeletal Muscles.	7
1.3	The organization of muscle.	8
1.4	Organization of actin and myosin within a muscle fiber.	9
1.5	Organization of the connective tissue within muscle.	10
1.6	The sliding filament model.	10
1.7	Actin and myosin filament sliding.	11
1.8	The Hill's three element model.	13
2.1	Perturbation and force plate machine.	15
2.2	Diagram of the force plate and the dorsiflexive stance of foot.	16
2.3	Dorsiflexive and plantarflexive position of the foot.	16
2.4	All the phases of the gait cycle.	18
2.5	The five sub-phases of the stance phase of the gait cycle.	18
2.6	The stance phase of the gait in percentages.	19
2.7	Graph of the full gait cycle	19
2.8	Visualization of the stance and swing phase.	20
2.9	The sub-phases of the swing phase of gait cycle.	20
2.10	The time dimensions of walking cycle.	21
2.11	The angle of the ankle with respect to the body.	23
2.12	Center of pressure displacement variability.	24
2.13	Ankle angle data averaged over trials.	25
2.14	The average of ankle angle with standard deviations.	26
2.15	The average of ankle angle with plantarflexive and dorsiflexive perturbations.	26
2.16	Ground reaction force in the x direction.	27
2.17	Ground reaction force in the z direction.	27
2.18	The average of ankle angle with various perturbations.	28
2.19	The average of ankle angle with various perturbations.	28
2.20	The average of ankle angle with various perturbations.	29
3.1	Normality test using <i>histfit</i>	36
3.2	PassingBablok regression fit for ankle angle.	37
3.3	PassingBablok residual plot for ankle angle.	37
3.4	PassingBablok linearity test for ankle angle.	38
3.5	The maximums in order of occurrence for no perturbation and the 2° plantarflexive perturbations.	39
3.6	The maximum for no perturbation compared against the 2° plantarflexive perturbations maximums	40

3.7	The slopes of the maximums for no perturbation and 2° plantarflexive perturbations. . .	40
3.8	The maximums in order of occurrence for no perturbation and the 2° plantarflexive perturbations.	41
3.9	The maximum for no perturbation compared against the 2° plantarflexive perturbations maximums	41
3.10	The slopes of the maximums for no perturbation and 2° plantarflexive perturbations. . .	42
3.11	The maximums in order of occurrence for no perturbation and the 2° plantarflexive perturbations.	42
3.12	The maximum for no perturbation compared against the 2° plantarflexive perturbations maximums	43
3.13	The slopes of the maximums for no perturbation and 2° plantarflexive perturbations. . .	43
3.14	The maximums in order of occurrence for no perturbation and the 2° plantarflexive perturbations.	44
3.15	The maximum for no perturbation compared against the 2° plantarflexive perturbations maximums	45
3.16	The slopes of the maximums for no perturbation and 2° plantarflexive perturbations. . .	45
3.17	Center of pressure of subject AB43 at 2°	46
3.18	Center of pressure of both perturbations at 350 ms and 2°	46
3.19	Center of pressure of subject AB122 at 5°	47
3.20	Center of pressure of both perturbations at 100 ms and 5°	48
3.21	Sine fitting for center of pressure of plantarflexive perturbation.	49
3.22	Curve fit on the non perturbed ankle angle data.	51
3.23	Curve fit for ankle data with 100 ms plantarflexive perturbation.	52
3.24	Curve fit for ankle data with 225 ms plantarflexive perturbation.	52
3.25	Curve fit for ankle data with 350 ms plantarflexive perturbation.	53

List of Tables

3.1	Ankle angle minimums and maximum at 2° perturbation.	31
3.2	Continuation of the ankle minimums and maximum at 2° perturbation.	32
3.3	Ankle angle minimums and maximum at 5° perturbation.	32
3.4	Ankle angle correlation coefficient at 2° perturbation.	33
3.5	Ankle angle correlation coefficient at 5° perturbation.	34

Chapter 1

Background

1.1 Biology of Musculoskeletal System

The human musculoskeletal system is an organ system that gives humans the ability to move, by using a combination of their muscular system and skeletal system. The musculoskeletal system provides good support, stability, and movement of the body. It is made up of the bones, muscles, cartilage, tendons, ligaments, joints, and other connective tissue that supports and binds tissues and organs together. The musculoskeletal system's primary functions include supporting the body, allowing motion, and protecting vital organs [30]. Fig. 1.1 shows the back anatomy of the human body, with the left side labeling the various muscles and the right labeling the various bones with relation to the muscles. Fig. 1.2 similarly shows the muscles and the bones on the front of the human anatomy.

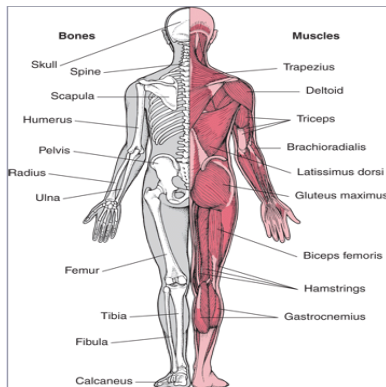


Figure 1.1: The layout of skeletal muscle on the back side of the human body, along with the bones [30].

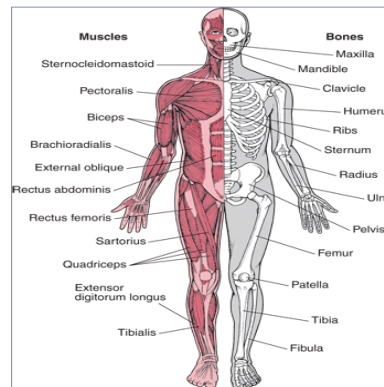


Figure 1.2: The layout of skeletal muscle on the front side of the human body, along with the bones [30].

There are three types of muscles: skeletal, smooth, and cardiac (heart). The skeletal and smooth muscles are part of the musculoskeletal system. The focus here is on the skeletal muscles, which are the type that contract to move the various parts of the body. Skeletal muscles are bundles of contractile fibers that are organized in a regular pattern, so that under a microscope they appear as stripes. Skeletal muscles, which are responsible for posture and movement, are attached to bones and arranged in opposing groups around joints. Muscles and bones work together to move the body. The muscles are attached to bones by bands of tough connective tissue called tendons. Movement occurs when muscles shorten or contract and pull rather than push on a bone. Muscles can only pull on a bone, not push. The skeleton can be moved by the coordinated action of pairs of muscles. One muscle will move a bone

in one direction while the other will move the bone in the opposite direction [36]. For example, muscles that bend the elbow (biceps) are countered by muscles that straighten it (triceps). These countering movements are balanced. The balance makes movements smooth, which helps prevent damage to the musculoskeletal system. Skeletal muscles are controlled by the brain and are considered voluntary muscles because they operate with a person’s conscious control [36].

Skeletal muscle is organized into bundles of muscle cells or fibers that are held together by a sheath of connective tissue. This enables the muscle cells to function together as a unit. Each muscle fiber is a single cell with many nuclei. Each fiber is comprised of many smaller myofibrils arranged lengthwise. The entire muscle, as well as the individual cells, are wrapped in collagen as shown in Fig. 1.3. Near the end, collagen fibers of a tendon merges with the perimysium and endomysium of the muscle. The collagen merges to form the tendons, which attach the muscle to the bone [39].

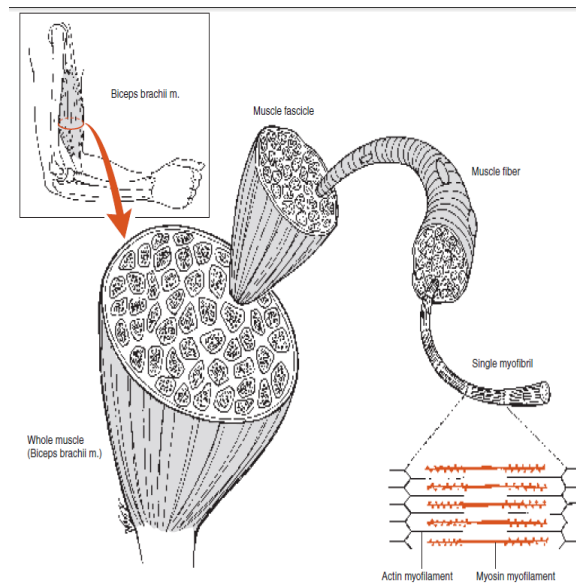


Figure 1.3: The organization of muscle. A progressive view of a whole muscle demonstrates the organization of the filaments that compose the muscle [30].

The functional unit that produces motion at a joint consists of two discrete units, the muscle belly and the tendon that binds the muscle belly to the bone. The muscle belly consists of the muscle cells, or fibers, that produce the contraction and the connective tissue encasing the muscle fibers. A skeletal muscle fiber is a long cylindrical, multinucleated cell that is filled with smaller units of filaments. These filamentous structures are roughly aligned parallel to the muscle fiber itself. The largest of the filaments is the myofibril, which takes up almost the entire cross section of the muscle fiber. Myofibrils are long, cylindrical strands of contractile proteins. Typically there are hundreds of these in one cross section of a muscle fiber. Looking at one myofibril, it is divided into segments called sarcomeres. Each sarcomere also contains filaments, known as myofilaments. These are the contractile units of a muscle. There are two types of myofilaments within each sarcomere. The thicker myofilaments are composed of myosin protein molecules, and the thinner myofilaments are composed of molecules of the protein actin. Sliding of the actin myofilament on the myosin chain is the basic mechanism of muscle contraction [30].

A dark stripe called a Z-line marks the ends of one sarcomere and the beginning of the next. Sarcomeres are composed of thick filaments and thin filaments. The thin filaments are attached at one end to a Z-line and extend toward the center of the sarcomere. The thick filaments, by contrast, lie at the center of the sarcomere and overlap the thin filaments. The thick and thin filaments slide

with respect to one another, using ATP as a source of energy. As a result of the sliding, the Z discs are pulled closer together. This is called the sliding filament mechanism. The contraction of a whole muscle fiber results from the simultaneous contraction of all of its sarcomeres [30].

1.2 The Mechanics of Muscle Movement

The sarcomere contains the contractile proteins actin and myosin, which is the basic functional unit of a muscle. Contraction of a whole muscle is the sum of singular contractions occurring within the individual sarcomeres. The thinner actin chains are more abundant than the myosin myofilaments in a sarcomere. The actin myofilaments are anchored at both ends of the sarcomere at the Z-line and project into the interior of the sarcomere where they surround a thicker myosin myofilament [35].

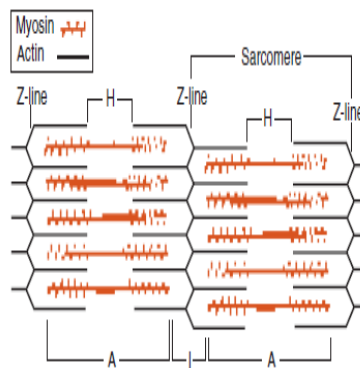


Figure 1.4: Organization of actin and myosin within a muscle fiber. The arrangement of the actin and myosin chains in two sarcomeres within a fiber give the characteristic of skeletal muscle [30].

The arrangement of myosin myofilaments surrounded by actin myofilaments as they are repeated throughout the sarcomere is shown in Fig. 1.4. The amount of these contractile elements within the cells is strongly related to a muscle’s contractile force. Contraction results from the formation of cross-bridges between the myosin and actin myofilaments, causing the actin chains to slide on the myosin chain [3]. The connective tissue consists of the epimysium surrounding the whole belly, the perimysium encasing smaller bundles of muscle fibers, and the endomysium that covers individual muscle fibers.

Fig. 1.5 gives a visual representation of how the muscles are composed. The outermost layer of connective tissue that surrounds the entire muscle belly is known as the epimysium. The muscle belly is divided into smaller bundles by more connective tissue known as perimysium. Finally, individual fibers are surrounded by more connective tissue, called the endomysium. Thus the entire muscle belly is contained in a large network of connective tissue that then is bound to the connective tissue tendons at the end of the muscle. The amount of connective tissue vary widely from muscle to muscle. The amount of connective tissue within an individual muscle influences the mechanical properties of that muscle. It shows the varied mechanical responses of individual muscles. An essential function of muscle is to produce joint movement. The passive range of motion (ROM) available at a joint depends on the shape of the articular surfaces as well as on the surrounding soft tissues [30]. However, the joint’s active ROM depends on a muscle’s ability to pull the limb through a joint’s available ROM. Under normal conditions, active ROM is approximately equal to a joint’s passive ROM. There is a wide variation in the amount of motion available at joints throughout the body. The knee joint is capable of flexing through an arc of approximately 140°, but the the thumb usually is capable of no more than about

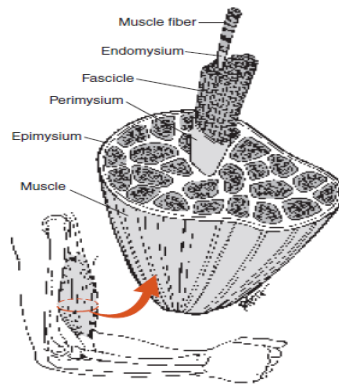


Figure 1.5: Organization of the connective tissue within muscle. The whole muscle belly is an organized system of connective tissue [30].

90° of flexion. Joints that exhibit large ROMs require muscles capable of moving the joint through the entire range. Thus muscles exhibit structural specifications that influence the magnitude of the excursion that is produced by a contraction. The length of the fibers composing the muscle and the length of the muscle’s moment arm are the main characteristics that determine the range of motion [30].

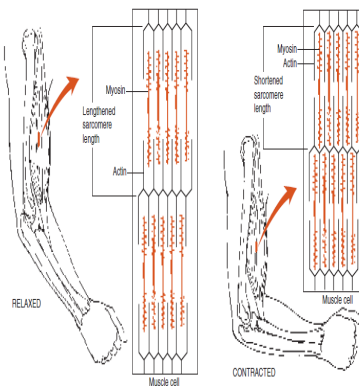


Figure 1.6: The sliding filament model. The contraction of skeletal muscle results from the sliding of the actin chains on the myosin chains. [30].

Fig. 1.6 shows that the tension of the contraction depends upon the number of cross-bridges formed between the actin and myosin myofilaments. The number of cross-bridges formed depends not only on the abundance of the actin and myosin molecules, but also on the frequency of the stimulus to form cross-bridges. Each myosin molecule is shaped like a golf club, with the head of the golf club pointed out from the surface of the thick filament as shown in Fig. 1.7. This structure will form the cross bridge that binds to the thin filament.

The calcium ions (Ca^{++}) flow into the sarcomere with its thick and thin filaments. This causes the filaments to start sliding and thus the sarcomere to shorten. But very quickly, the Ca^{++} is actively transported back into the sarcoplasmic reticulum and the sarcomere relaxes. Actin is the main protein of the thin filament. A second protein, troponin, is found at intervals. When Ca^{++} binds to troponin, this allows myosin heads to bind to the actin of the thin filament, creating cross bridges. The cross bridges then pull on the thin filaments, causing the sarcomere to shorten. The cross bridges then release

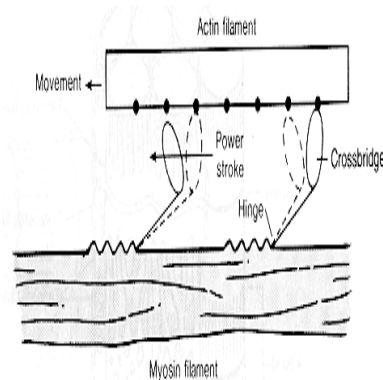


Figure 1.7: Muscle shortening corresponds to the sliding of actin filaments past myosin filaments.

the actin, with ATP used by each cross bridge in each cycle. When Ca^{++} is present, this cycling of cross bridges continues and the filaments continue to slide with respect to one another. When Ca^{++} goes back into the sarcoplasmic reticulum, the contraction stops [3].

1.3 Hill's Model

Muscle produces two kinds of force, active and passive, which sum to create a muscle's total force. A muscle's contractile elements provide its active force through the actin and myosin mechanism. Non-contractile elements contribute to its passive force. A muscle's passive element has properties which are elastic, but it can be modeled more simply as a spring. Because this spring-like element attaches in series with the contractile element, the force that the contractile element produces is an active force. This force is transmitted to the skeleton by a series elastic element. Muscles, however, have another elastic element, as well, called a parallel elastic element that also contributes to its passive force [37].

Activated muscles produce more force when held isometrically, which is at a fixed length, than when they shorten. When muscles shorten, they waste some of their active force in overcoming an inherent resistance. This resistance is not from the series elastic element. The faster a muscle shortens the less total force it produces. Assuming a constant active force, the faster shortening leads to a larger resistive force. To account for the fact that muscle produces less force when it shortens, this viscous element is proposed which lies in parallel with the contractile element. This component is called a parallel elastic element [32].

The force-velocity relationship was first described by A. V. Hill (1938). Hill developed a rectangular hyperbolic equation to describe the muscle force-velocity relationship. This relation that describes the force-velocity behavior of muscles during shortening is the Hill's equation. This is a state equation applicable to skeletal muscle and is used to show tetanic contraction. It relates tension to velocity as follows:

$$(P + a)v = b(P_0 - P), \quad (1.1)$$

where a and b are constants derived experimentally (usually $a = 0.25$, $b = 0.25$), P is muscle force, P_0 is maximum tetanic tension, and v is muscle velocity.

Another form of the Hill's equation can be expressed as

$$(P + a)(v + b) = b(P_0 + a), \quad (1.2)$$

where v is the speed of a muscle contraction under a load P , P_0 is the maximum value of the isometric force during tetanic stimulation of the entire muscle, and constants a and b are empirical values. The constant a has the dimensionality of force and is equal to about 4×10^5 dynes/cm of a cross section of various types of muscles, while the constant b has the dimensionality of velocity, expressed in cm/sec or L_0/sec , where L_0 is the initial length of the muscle. The second constant differs for various muscles [2].

If the contracting muscle has a length L at the moment t , then the velocity of its contraction $\frac{\partial L}{\partial t}$ is determined by the formula

$$\frac{\partial L}{\partial t} = \frac{(F_1 - F)b}{(F + a)} \quad (1.3)$$

where F is the force that overcomes the muscle, F_1 is the maximum force of the muscle at the length at which the velocity of its contraction is measured, and a and b are constants.

Hill's equation accurately describes the contraction of muscles in vertebrates and invertebrates, although the correlation of the constants of the equation to the contractile, elastic, and viscous elements in the muscle structure has not yet been established.

The Hill's equation demonstrates that the relationship between P and v is hyperbolic. Therefore, the higher the load applied to the muscle, the lower the contraction velocity. Similarly, the higher the contraction velocity, the lower the tension in the muscle. This hyperbolic form has been found to fit the empirical constant only during isotonic contractions near resting length. In an isotonic contraction, tension remains unchanged and the muscle's length changes. For example, an isotonic contraction is lifting an object at a constant speed. There are two types of isotonic contractions: concentric and eccentric. In a concentric contraction, the muscle tension rises to meet the resistance, then remains the same as the muscle shortens. In eccentric, the muscle lengthens due to the resistance being greater than the force the muscle is producing [4]. The muscle tension decreases as the shortening velocity increases. This feature has two main causes. The major cause appears to be the loss of tension in the cross bridges in the contractile element and then they reform in a shortened condition. The second cause appears to be the fluid viscosity in both the contractile element and the connective tissue. Whichever the cause of loss of tension, it is a viscous friction and can therefore be modeled as a fluid damper.

Muscle velocity affects force development in whole muscles. Force (P) is greater during lengthening than shortening contractions. The greater the shortening velocity (v), the smaller the force, which is why humans cannot lift heavy objects quickly. In the shortening regime, mechanical power output is maximum when P and v are around one-third their maximum values [32].

Muscle produces two kinds of force, active and passive, which sum to compose a muscle's total force. A muscle's contractile elements provide its active force through the actin and myosin mechanism. Non-contractile elements contribute to its passive force. A muscle's passive element has properties which are elastic, but it can be modeled more simply as a spring. Because this spring-like element attaches in series with the contractile element, the force that the contractile element produces is an active force transmitted to the skeleton via a series elastic element. Muscles, however, have another elastic element, as well, called a parallel elastic element that also contributes to its passive force.

The three-element Hill's muscle model is a representation of the muscle mechanical response. The model is constituted by a contractile element (CE) and two non-linear spring elements, one in series (SE) and another in parallel (PE). The active force of the contractile element comes from the force generated by the actin and myosin cross-bridges at the sarcomere level. It is fully extensible when inactive but capable of shortening when activated. The connective tissue that surround the contractile element influences the muscle's force-length curve. The PE represents the passive force of these connective tissues and has a soft tissue mechanical behavior. The PE is responsible for the muscle passive

behavior when it is stretched, even when the contractile element is not activated. The SE represents the tendon and the elasticity of the myofilaments. It also provides an energy storing mechanism [32].

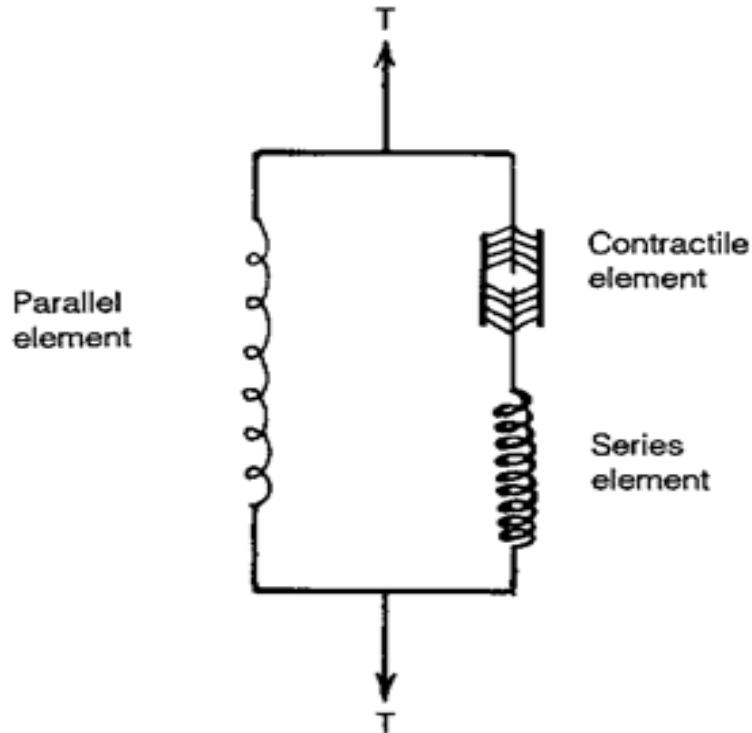


Figure 1.8: The Hill’s functional model of the muscle. The three element model with the parallel element, contractile element, and series element [20].

In Fig. 1.8, the fundamental assumptions were that the resting length–tension relation is governed by an elastic element in parallel with a contractile element. This means that active and passive tensions add. The parallel elastic element is the passive property. Also, the active contractile element is determined by active length–tension and velocity–tension relationships only. The series elastic element becomes evident in quick–release experiment [20].

Resting length–tension relation is governed by an elastic element in parallel with a contractile element. The active and passive tensions add together. The parallel elastic element is the passive property. The active contractile element is determined by active length–tension and velocity–tension relationships only. The net force–length characteristics of muscle is a combination of the force–length characteristics of both active and passive elements. The forces in the contractile element, F_{CE} , including the series element, F_{SE} , and the parallel element, F_{PE} , satisfy the following equation

$$F = F_{PE} + F_{SE}, \quad (1.4)$$

and

$$F_{CE} = F_{SE}. \quad (1.5)$$

During the isometric contraction, the series elastic component is under tension and therefore it is stretched a certain amount. Since the overall length of the muscle is kept constant, the stretching of the series element can only occur if there is an equal shortening of the contractile element itself [32].

1.4 Measuring Stiffness

Stiffness is the rigidity of an object. It is the amount to which the body resists deformation in response to an applied force. The complementary idea is flexibility. The relationship between the two concepts is that the more flexible an object is, the less stiff it is. The stiffness (k) of a body is a measurement of the resistance of an elastic body to deformation. k is usually measured in Newtons per meter. The equation for stiffness where a body has a single degree of freedom, such as stretching or compressing a rod, is

$$k = F/\lambda \tag{1.6}$$

where F is the force applied on the body in Newtons, λ is the displacement produced by the force along the same degree of freedom in meters, and k is the stiffness coefficient measured in Newtons per meter [15].

It is noted that for a body with multiple degrees of freedom, the equation above does not apply since the applied force generates not only the deflection along its own direction, but also those along other directions.

The body can also have rotational stiffness, \mathcal{K} . The equation for rotational stiffness is

$$\mathcal{K} = M/\theta \tag{1.7}$$

where M is the applied moment in Newton meters, and θ is the rotation in radians. The rotational stiffness is measured in Newtons–meters per radian [15].

Chapter 2

Data Introduction

2.1 The Origin of the Data

The data was gathered in a study by Gregg et al [16]. Thirteen able-bodied subjects between the ages of 18 to 70 years were used for the study. The individuals were excluded if they had a body weight was over 250 pounds, were pregnant, had a history of back and leg injury, had joint problems, or any other illnesses that could interfere with the data. Subjects were provided a harness and handrails to protect them from falls. The harness did not provide body-weight support, and the subjects were instructed not to use the handrails unless they lost balance, which rarely occurred. Each subject was measured with an electrogoniometer that measured the ankle angle. Data were recorded synchronously with a 1 kHz sampling rate. A force plate was mounted on top of the perturbation device as shown in Fig. 2.1 to measure the forces exerted by the stance foot, which is the foot that is in the stance phase of the gait cycle [16].

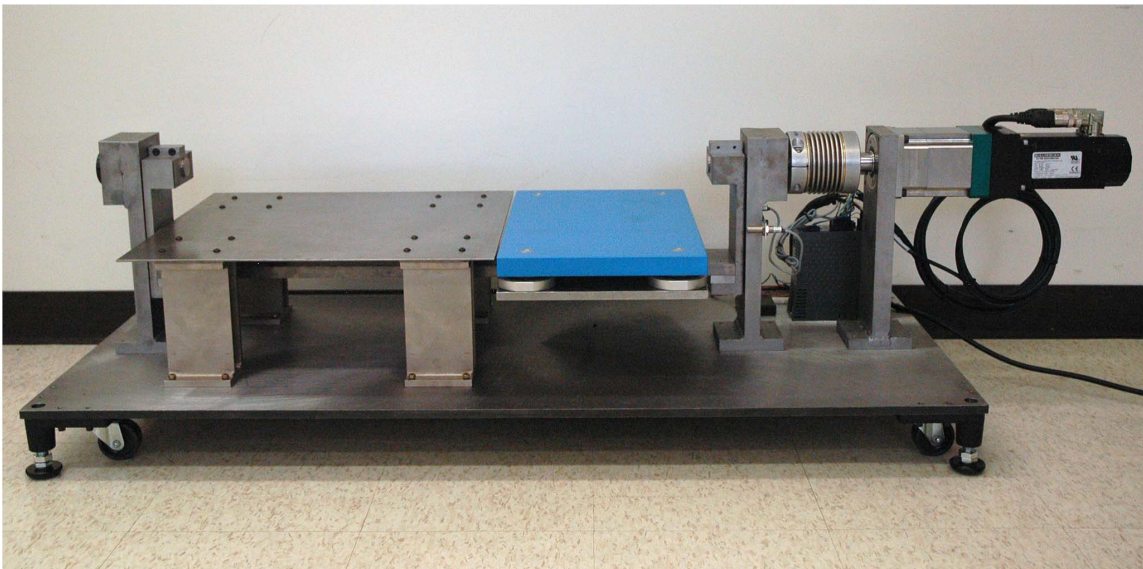


Figure 2.1: Perturbation and force plate machine that was used to collect the data used in this study [16].

As seen in Fig. 2.1, the perturbation device was placed within an elevated walkway to make an even walking surface. Each trial consisted of the subject walking along the walkway, stepping on the force

plate (in blue), and walking a few more steps on the walkway and then stopping.

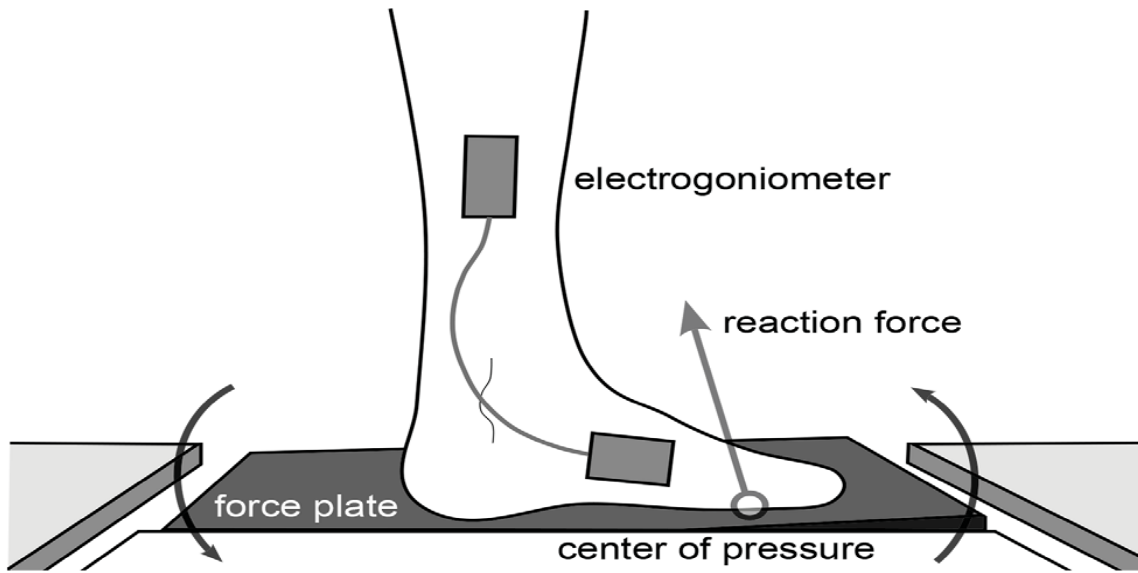


Figure 2.2: Diagram of robotic force plate and the dorsiflexive stance of the foot with center of pressure and ground reaction force [16].

Subjects were asked to walk at a comfortable speed, and a metronome was used to reduce step period variability and encourage a walk between 85–90 steps per minute for consistency. The starting location of each subject was adjusted such that, on average, the center of rotation of the ankle at heel contact aligned with the rotational axis of the perturbation platform. Perturbations occurred in 50% of the trials to make them unpredictable. The 2° perturbations consists of the force plate tilting 2° either in the plantarflexive position (down) or dorsiflexive position (up) at a specific time as shown in Fig. 2.3. The 5° perturbations are the same except the force plate tilts at a 5° angle. For the 2° study, perturbations were timed at different points after ipsilateral heel strike (100, 225, 350, or 475 ms with equal probability) to eliminate bias. The 475 ms condition was excluded because the foot occasionally lifted off the platform before the perturbation was completed. Each set of trials had a fixed number of perturbations, where each time point was tested 10 times in a random order.

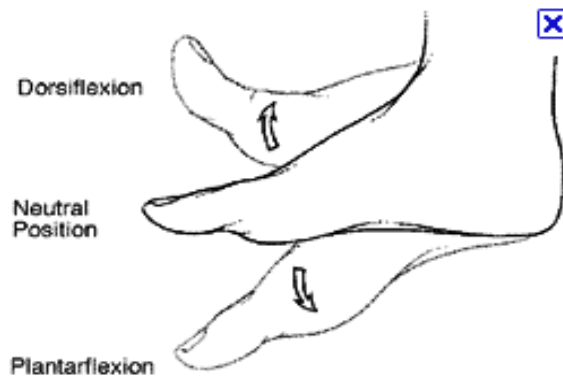


Figure 2.3: The foot in the neutral, plantarflexive and dorsiflexive positions [21].

Dorsiflexion and plantarflexion refers to extension or flexion of the foot at the ankle. These terms

refer to flexion between the foot and the front of the leg. Dorsiflexion is where the toes are brought closer to the shin, the turning of the foot or the toes upward. This decreases the angle between the dorsum of the foot and the leg. For example, when walking on the heels the ankle is described as being in a dorsiflexive position. Plantarflexion is the movement which decreases the angle between the sole of the foot and the back of the leg. It is the pointing of the foot and toes. For example, standing on the tiptoes can be described as plantarflexion.

The perturbation direction (dorsiflexion or plantarflexion) was chosen at random with equal probability to prevent anticipatory compensation from the subjects. There was a total of 400 perturbation trials and approximately 400 unperturbed trials in the 2° study. This large number of trials is to minimize inter-subject variability and allow a small number of subjects to be used. The experiment was repeated with 5° perturbations. The 5° experiment had fewer subjects and invoked only the 100 ms perturbation condition. These experiments entailed 100 perturbed trials and approximately 100 unperturbed trials [16]. Data for both experiments are available from the Dryad Digital Repository [17]. The data used contains only the stance phase. The measurements are in the sagittal plane with respect to the ankle's center of rotation. The sagittal plane is the plane that divides the body of a bilaterally symmetrical animal into right and left sections.

The perturbations occurred once at the given time point (ms). For the plantarflexive perturbation, the platform tilted down away from the test subject walking, and for the dorsiflexive perturbation, the platform tilted towards the subject, with respect to the pivot point in the middle of the platform.

2.2 Locomotion and Gait

Locomotion is defined as a progression of the body as a whole produced by movements of the body segments. During normal walking, body weight is supported by one limb and this part of the walk demonstrates several capabilities such as muscular coordination, balance, strength and joint kinematics. Gait is the medical term to describe human locomotion, which is the way humans walk. Normal gait is a series of rhythmic alternating movements created by alternating propulsion of the legs, which creates forward movement. In total, it is the movement of the lower limbs, upper limbs with the trunk leading to forward progression of the center of gravity [22]. To have gait, there needs to be the ability to support upright position, the ability to maintain balance, and the ability to create a new step forward. The forces for gait are muscular force, gravitational force, forces of momentum, and floor reaction force. Fig. 2.4 shows the gait cycle color coded for the different phases.

The gait cycle begins when one foot contacts the ground and ends when that foot contacts the ground again. Thus, each cycle begins at initial contact with a stance phase and proceeds through a swing phase until the cycle ends with the limb's next initial contact. Stance phase accounts for approximately 60%, and swing phase for approximately 40%, of a single gait cycle. Each gait cycle includes two periods when both feet are on the ground. The first period of double limb support begins at initial contact, and lasts for the first 10 to 12 percent of the cycle. The second period of double limb support occurs in the final 10 to 12 percent of stance phase. As the stance limb prepares to leave the ground, the opposite limb contacts the ground and accepts the body's weight. The two periods of double limb support account for 20 to 24 percent of the gait cycle's total duration [27].

The gait cycle starts with the stance phase. It is divided into 5 sub-phases shown in consecutive order in Fig. 2.5, which include initial contact, loading response, mid-stance, terminal stance, and pre-swing. Those subphases are characterized as heel strike to foot flat (0–10% of gait cycle), foot flat through mid-stance (10–30% of gait cycle), mid-stance through heel off (30–50% of gait cycle), and heel off to toe off (50–60% of the gait cycle).

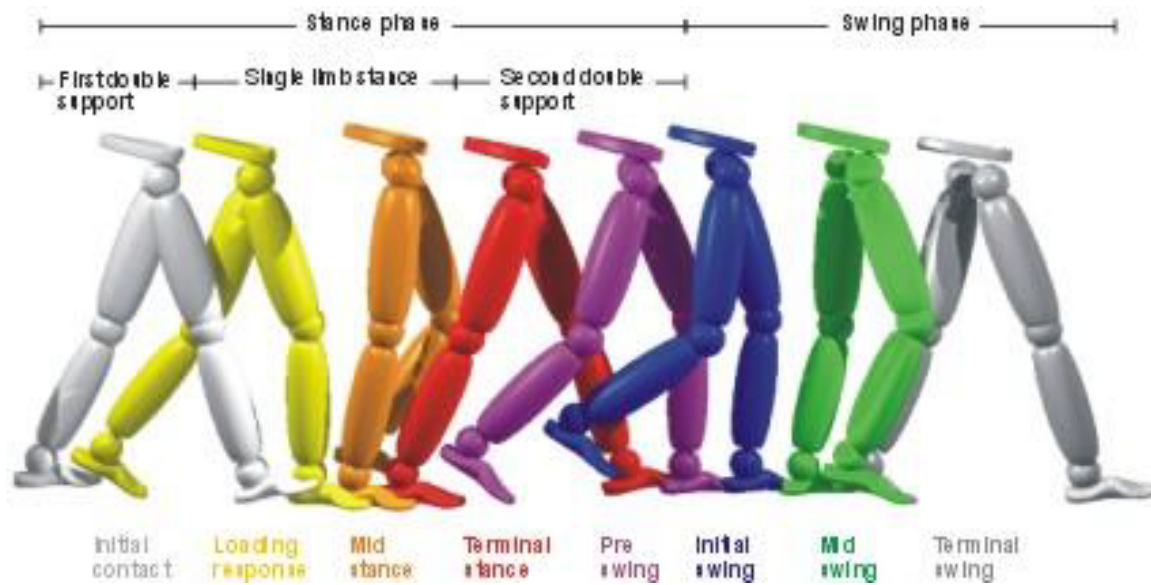


Figure 2.4: All the phases of the gait cycle [27].

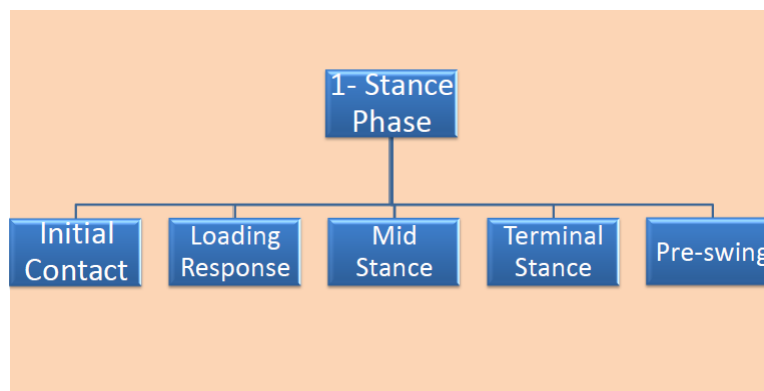


Figure 2.5: The five sub-phases of the stance phase of the gait cycle [27].

The stance phase begins at the instance that one extremity contacts the ground and continues only as long as some portion of the foot is in contact with the ground. It is initial contact, which is heel strike to no contact, which is toe off. Stance phase begins at the instance that one foot contacts the ground, which is the initial contact made by heel strike, and continues as long as some portion of the foot is in contact with the ground. The phase ends when that foot lifts off the ground: toe off. The stance phase is the weight bearing phase. Fig. 2.6 incorporates the percentages of the stance phase of gait. It provides the stability of the gait, and it is necessary for an accurate swing phase to take place [22]. Fig. 2.7 shows the full cycle of the gait as a graph.

At the initial contact of the stance phase which is heel strike, the stance phase begins with initial contact and ends with the foot flat. The knee is extended and the ankle is neutral or slightly plantarflexed. Normally, the heel contacts the ground first. This phase continues until the foot is flat on the ground [22].

The loading response subphase, which is foot flat, occurs immediately following heel strike. It is the point at which the foot fully contacts the floor. It corresponds to the gait cycle's first period of double limb support and ends with contralateral toe off, when the opposite foot leaves the ground. During

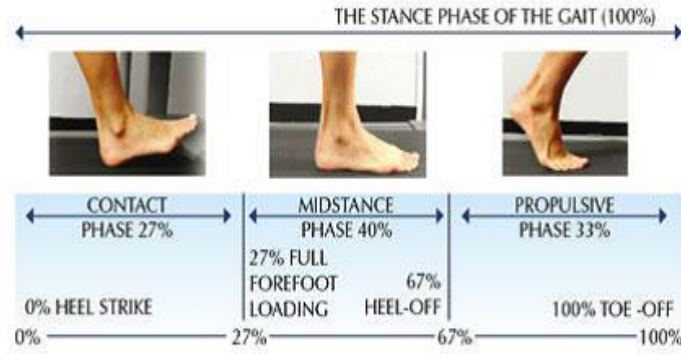


Figure 2.6: The stance phase of the gait in percentages divided into three parts, the contact phase 27%, midstance phase 40% and the propulsive phase 33% [27].

this, the knee flexes 15° while the ankle plantarflexes 15° , as an energy-conserving mechanism [33].

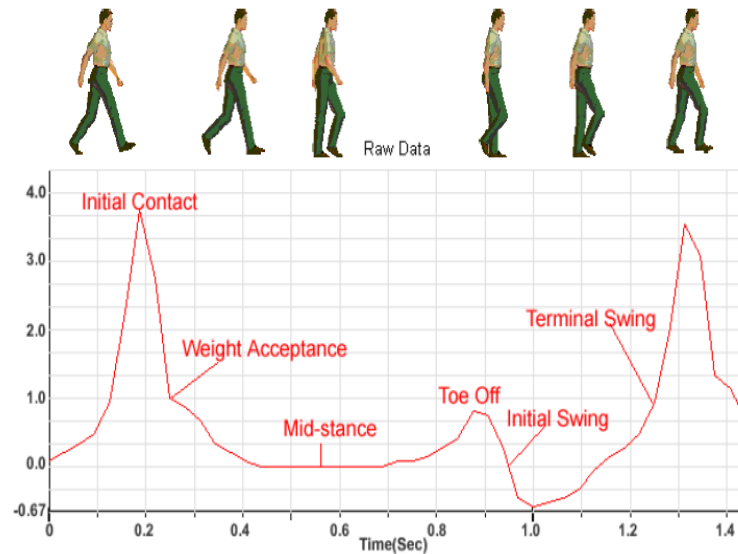


Figure 2.7: Graph of the full gait cycle [27].

The next phase is the mid-stance phase. This phase represents 30% of the gait cycle, during which the body passes directly over the supporting foot as the body comes forward. This is where the foot supports the body weight of the human. The foot is flat on the floor in a stable position. The body is carried forward over the stance foot with the hip extending and the foot gradually placed on the floor. This phase begins with contralateral toe off and ends when the center of gravity is directly over the reference foot. By mid-stance, the knee is extended and the ankle is neutral again. This phase ends as the body weight passes forward eventually forcing the heel to rise [27].

The next sub-phase of the stance phase is the terminal stance, which is heel off. The terminal stance follows the midstance at which time the heel rises until the other foot makes contact with the floor. During this phase the body weight moves ahead of the forefoot. The heel is raised as the body moves forward over the stance foot. The hip is in the full extension, internal rotation and adduction. This corresponds to the knee extending [22].

The last subphase is the pre-swing, which is toe off. It is the point following heel off where only the toes of the supporting foot is in contact with the ground. It is the final double support stance period which is defined from the time of the initial contact with the contralateral foot to the ipsilateral toe-off. The double support is when the lower limb of one side of the body is beginning its stance phase and the opposite side is ending its stance phase. During double support both the lower limbs are in contact with the ground at the same time. However, this phase is absent in running [33]. Fig. 2.8 gives another visualization of how the ankle moves during all the subphases.

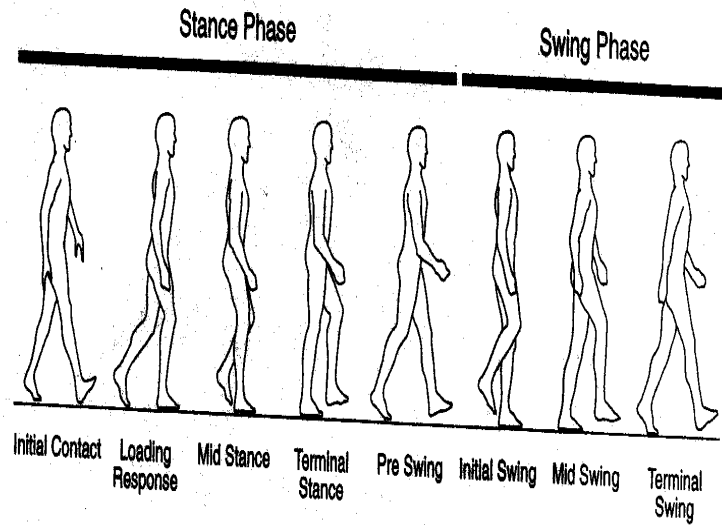


Figure 2.8: Visualization of the stance and swing phase and all of the subphases corresponding to each pose [33].

The next phase of the gait cycle is the swing phase. It makes up 40% of the normal gait cycle. It begins as soon as the big toe of the one foot leaves the ground (after toe-off) and finishes just prior to heel strike or contact of the same foot. This phase includes initial swing, mid swing and terminal swing as shown in Fig. 2.9.

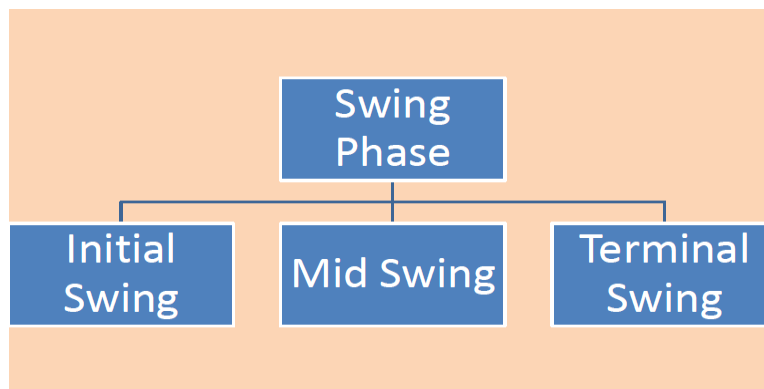


Figure 2.9: The three sub-phases of the swing phase of the gait cycle [27].

The initial swing is the acceleration of the body. It is the initial third of the swing phase from 60–73% of the gait cycle. It begins once the toe leaves the ground and continues until mid swing, or

the point at which the swinging extremity is directly under the body. Forward momentum is provided by the ground reaction to the push-off action, which is when the heel is off the ground but the toes are in strong contact with the ground. This phase continues until maximum knee flexion occurs. The flexion of the knee is necessary for the swinging foot to clear the ground as it moves forward [27].

The mid-swing is the middle third of the swing phase from 73–87% of the gait cycle. It occurs approximately when the extremity passed directly beneath the body, or from the end of acceleration to the beginning of deceleration. Also, it can be defined from maximum knee flexion until the tibia is in vertical position. It begins the maximum knee flexion when the swing foot is under the body until the swing limb passes the stance limb and the tibia becomes in a vertical position [27].

The terminal swing sub-phase is the deceleration. The terminal swing is the final third of the swing phase from 78–100% of the gait cycle. It occurs after mid swing when the limb is decelerating in preparation for heel strike. It is defined from the time when the tibia is in vertical position to just before initial contact. The momentum slows down as the limb moves into the stance phase again. The knee is extending in preparation for the heel strike. The foot is in neutral position. As the heel touches the ground, the foot moves into plantarflexion [33]. Fig. 2.10 gives a full representation of the walking cycle with the percentages.

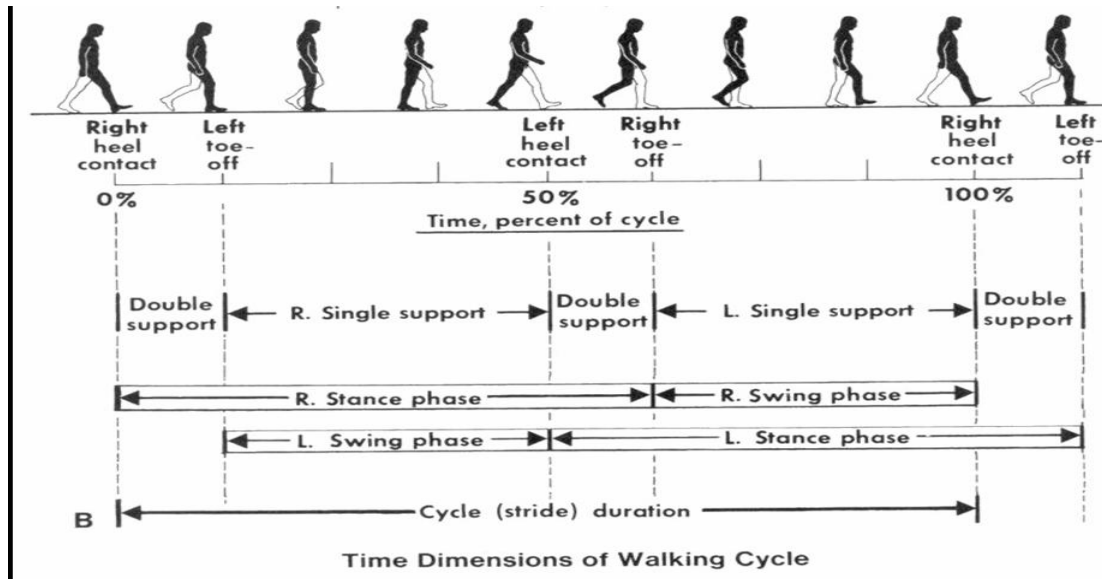


Figure 2.10: The diagram representing the gait cycle and the percentages of the phases and properties of the gait [33].

The movement pattern that happens during walking results from the interaction between external forces, such as joint reaction and ground reaction and the internal forces, such as the ones produced by muscles and other soft tissue. The ground reaction is helpful to understand how the muscle activity and timing contributes to stability and propulsion. The ground reaction force is equal in magnitude and opposite in direction to the force that the body exerts on the supporting surface with the foot. During the loading response, the ground reaction force produces a plantarflexion moment at the ankle joint. During mid-stance, ground reaction force produces a dorsiflexor moment at the ankle joint, as well as during the terminal stance and the pre-swing [33].

There are two variables which provide a basic description of the human gait: time and distance variables. The factors that affect variables are age, gender, height, size, distribution of mass, joint mobility, muscle strength, type of clothing and footwear, habit and psychological status. The stance

time is the amount of time that elapses during the stance phase of one extremity in a gait cycle [22]. Single-support time is the amount of time that elapses during the period when only one extremity is on the supporting surface in a gait cycle. Double-support time is the amount of time spent with both feet on the ground during one gait cycle. The percent of time spent is increased in elderly people and in those with balance disorders. The percentage of time spent decreases as the speed of walking increases. Stride length is the linear distance from the heel strike of one lower limb to the next heel strike of the same limb. Step length is the linear distance from the heel strike of one lower limb to the next heel strike of the opposite limb. Stride duration refers to the amount of time taken to accomplish one stride. Stride duration and gait cycle duration are synonymous. For a normal adult, one stride is approximately 1 second. Step duration is measured in seconds per step. Walking velocity is the rate of forward motion of the body. It is measured in meters/minute or cm/second [22].

$$\text{Walking Velocity}(\text{meters/second}) = \text{Distance Walked}(\text{meters})/\text{Time}(\text{sec}) \quad (2.1)$$

Free speed of gait refers to a person's normal walking speed. Slow and fast speed of gait refers to the speed slower or faster than the person's normal walking speed. Vertical displacement of the gait is a rhythmic up and down movement. The highest point is the midstance, and the lowest point is the double support. The average displacement is about 5 cm. The path is an extremely smooth sinusoidal curve. Lateral displacement is a rhythmic side to side movement. The lateral limit is mid stance. The average displacement is 5 cm. Again the path is a smooth sinusoidal curve. Overall, displacement is the sum of vertical and horizontal displacements [22].

2.3 Parameters

Movements of the ankle are important for normal coordinated gait. The angle of the ankle during the walking cycle can be measured. Fig. 2.11 shows the angles (θ) of the joints. The absolute angle is the orientation of a segment in space, which is the angle of inclination of a body segment. Segment angles are referred to as absolute angles measured from the right horizontal placed at the distal end of the segment. The segment angles include foot angle, shank angle, thigh angle and trunk angle. The relative angle is the joint angle, which is the included angle between the longitudinal axes of the two adjacent segments. The joint angles are ankle angle, knee angle, and hip angle [25]. In this study, the movements of dorsiflexion and plantarflexion of the ankle were evaluated. Dorsiflexion and plantarflexion refers to the ankle angle extesions mentioned in Section 2.1.

The relative angles can be determined from the absolute angles.

$$\theta_{ankle} = \theta_{shank} + (180 - \theta_{foot}) \quad (2.2)$$

The most important mechanism to smooth the gait pathway is foot and ankle motion. At initial contact, the ankle is elevated due to the heel lever arm but falls as the foot becomes plantar grade. At heel rise, the ankle again is elevated, which continues through terminal stance and pre-swing. These ankle motions, coordinated with the knee and controlled by muscle action, smooth the pathway of the center of mass during stance phase. The controlled lever arm of the forefoot at pre-swing is particularly helpful as it rounds out the sharp downward reversal of the center of mass. Thus it does not reduce a peak displacement period of the center of mass but rather smooths the pathway. Foot and ankle motion thus facilitate the path of the center of gravity, keeping it relatively horizontal throughout stance phase.

The center of pressure (COP) is the point of application of the ground reaction force vector. COP is the point of location of the vertical ground reaction force vector. When both feet are in contact with

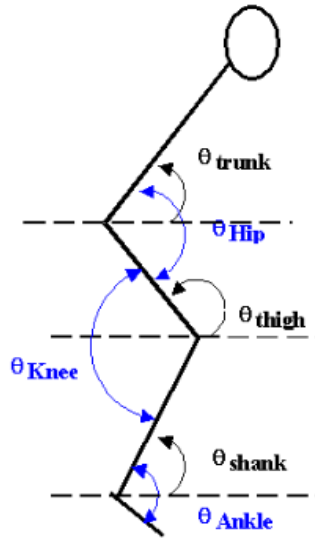


Figure 2.11: The angle of the ankle with respect to the body [25].

the ground, the location of COP under each foot reflects the neural control of the ankle muscles. COP moves to the anterior with the increased plantarflexion of the ankle. The ground reaction force vector represents the sum of all forces acting between a physical object and its supporting surface. Analysis of the center of pressure is common in studies on human postural control and gait. It is thought that changes in motor control may be reflected in changes in the center of pressure. The effect of some experimental condition on movement can be quantified by the changes in the center of pressure. During human walking, the center of pressure is near the heel at the time of heel-strike and moves anteriorly throughout the step, being located near the toes at toe-off [38].

COP measurements are gathered through the use of a force plate. A force plate collects data in the anterior-posterior direction (x-axis, forward and backward), the medial-lateral direction (y-axis, side-to-side) and the vertical direction (z-axis), as well as moments about all 3 axes. Together, these can be used to calculate the position of the center of pressure relative to the origin of the force plate. In this case, the COP data is in the x-axis and the z-axis. COP and Center of Gravity (COG) are both related to balance in that they are dependent on the position of the body with respect to the supporting surface. Center of gravity is subject to change based on posture. Center of pressure is the location on the supporting surface where the resultant vertical force vector acts [38].

A shift of COP is an indirect measure of postural sway and thus a measure of a person's ability to maintain balance. All people would sway in the anterior-posterior direction (forward and backward) and the medial-lateral direction (side-to-side) when they are simply standing still. This is a result of small contractions of muscles in the body to maintain an upright position. An increase in sway is not necessarily an indicator of poorer balance so much as it is an indicator of decreased neuromuscular control, although the postural sway occurs prior to a fall.

Fig. 2.12 shows center of pressure patterns during a normal stride in the x-axis direction during a normal stride. The upward projection of the COP is used as an estimate for the body center of mass (COM). Another reason for obtaining COM is for evaluating the ankle postural stiffness. This evaluation requires determining moment produced at the ankle for maintaining posture. The study used the moving average of the COP as an estimate for COM [23].

Ground reaction force (GRF) data is obtained from a force plate, which is attached to the walking

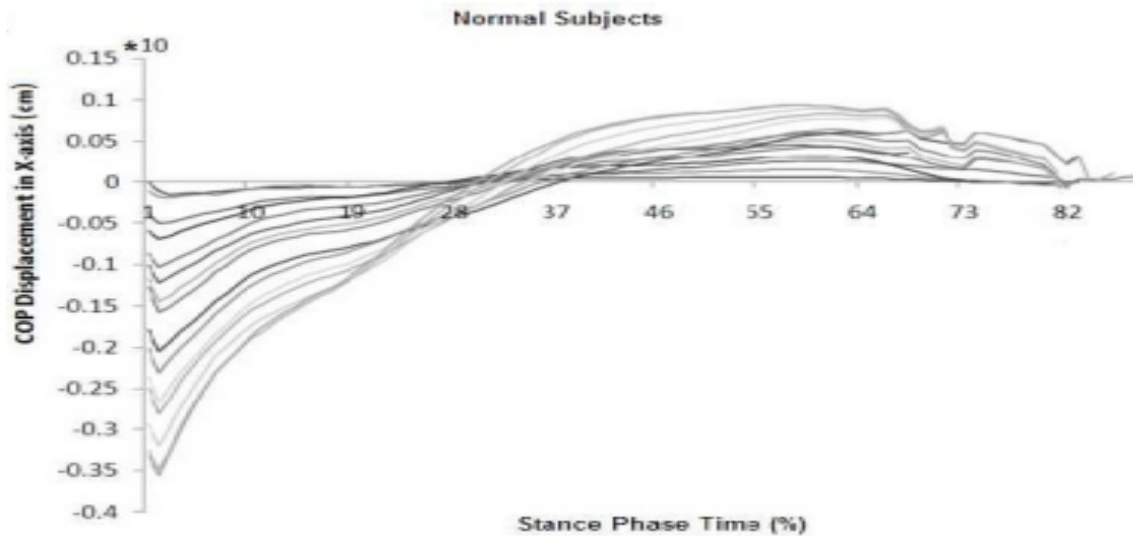


Figure 2.12: Center of pressure displacement in the x-axis with the variability of different test subjects [5].

platform. The GRF is the force exerted by the ground on a body in contact with it. A person standing motionless on the ground exerts a contact force on the ground, which is equal to the person’s weight, and at the same time an equal and opposite ground reaction force is exerted by the ground on the person. The GRF also has a component parallel to the ground, a motion that requires the exchange of horizontal forces with the ground, when the person is walking. The component of the GRF parallel to the surface is the frictional force. The ratio of the magnitude of the frictional force to the normal force yields the coefficient of static friction. GRF is often observed in people’s gait [40].

2.4 Data

The following diagrams are the graphs of the current data that was introduced in Section 2.1. There is a vast variety of data from the conducted experiment. It includes ankle angle, COP, GRF, and platform angle data sets; each with no perturbations as well as perturbations at each level (100 ms, 225 ms 350 ms) in plantarflexive and dorsiflexive perturbations.

All the data in these following graphs are from the normalized ankle angle data averaged over all trials for a single patient.

In Fig. 2.13, it is noticeable how the ankle angle changes in the stance phase of the gait cycle. The characteristics of an ankle are divided into two parts of the gait: the plantarflexion and the dorsiflexion. Plantarflexion is when the ankle is “bent down” and dorsiflexion is when the ankle is “raised up”. The ankle plantarflexes during the loading response. Then, it dorsiflexes gradually during mid stance. Afterwards, it plantarflexes during terminal stance. At the end, it starts to slightly plantarflex, which is when the ankle transitions into the swing phase. The negative values correspond to plantarflexion while the positive values correspond to the dorsiflexion. The zero ankle position was assigned to the position at which the foot was perpendicular to the shank of the leg. It is visible that the ankle changes direction at approximately 60 ms, and then again much more gradually at 600 to 700 ms until

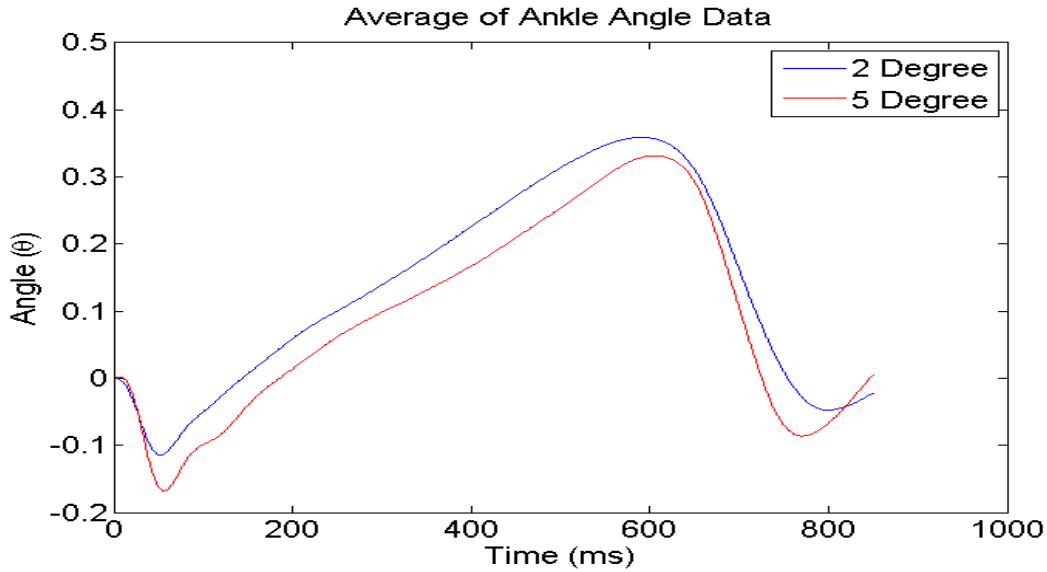


Figure 2.13: The normalized ankle angle data for a single patient averaged over all trials at 2° and 5° with no perturbation.

800 ms.

The ankle angle in the stance phase has 3 sections in the graph. The loading response, which is 0–10% of the gait cycle and 0–16.66% of the stance phase, is the first section. It is the period from initial contact until contralateral toe off. The mid-stance and terminal stance, which is from 10–50% of the gait cycle and 16.66–66.66% of the stance phase, is the second section. It ends when the opposite foot contacts the ground. The preswing, which is 50–60% of the gait cycle and 66.66–100% of the stance phase, is the last section. Fig. 2.13 shows those three sections as the line segments of different slopes. In Fig. 2.14, notice how as the stance phase proceeds the standard deviation grows, similar to the standard deviation growth for 5° perturbations. In Fig. 2.15, both the plantarflexive and dorsiflexive perturbations are shown. They are symmetric about the non-perturbed curve. They both show the reaction of the perturbations but in different directions.

Fig. 2.16 is the ground reaction force in the x direction for one subject averaged over all the trials. The blue curve is the 2° perturbation and the red curve is the 5° perturbation. Notice how there are dips in the graph. Those signify stages of the gait cycle. The data starts with heel contact. The first minimum is where the toes touch the platform and proceed to go into midstance. The maximum that is in the data is the end of the midstance where the heel is off. The data end with toe off. These local minima and maxima are specific subject to subject and importantly chance due to the perturbations.

Similarly, Fig. 2.17 shows the change in the curves. The first maximum is now the beginning of midstance and the second maximum is the end of midstance and the start to heel off. The local minimum is the transition of the midstance as the body travels over the foot. This is due to the GRF in the z direction. The GRF_x and GRF_z graphs are different in that they represent different axes. However, they both show the characteristic subphases of the gait.

From Fig. 2.13, Fig. 2.16, Fig. 2.17, the data for 2° non perturbed data has the same trend and pattern as the 5° non perturbed data. This leads to comparison of the perturbations at various time points of the data on a subject to subject basis.

In Fig. 2.18, notice how the angle is increased after the perturbations occurred compared to the rest of the uniform pattern. The ankle slightly dorsiflexes and then continues on its normal characteristic of

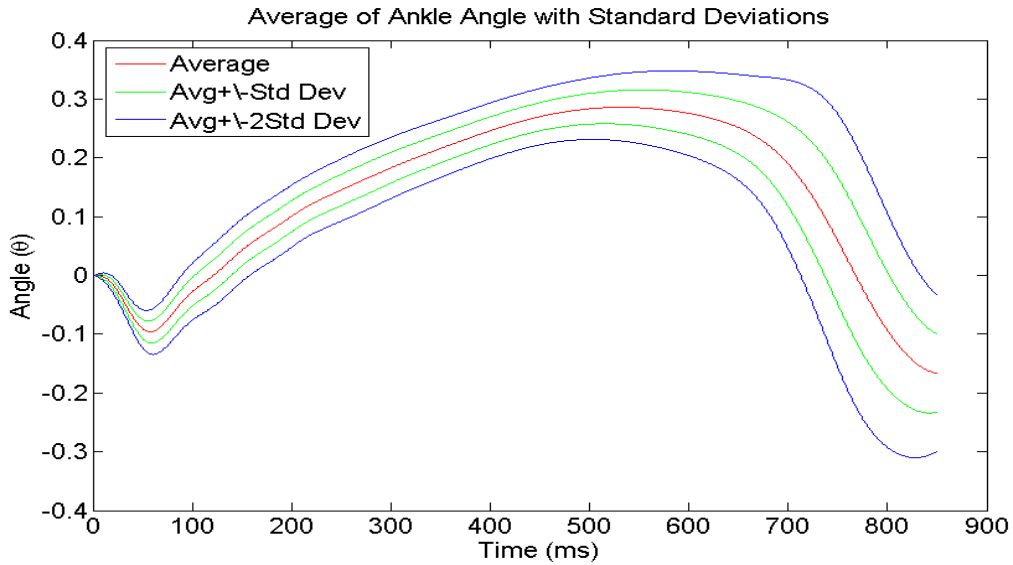


Figure 2.14: The normalized average of the ankle angle with one and two standard deviations at 2° tilt of the force plate.

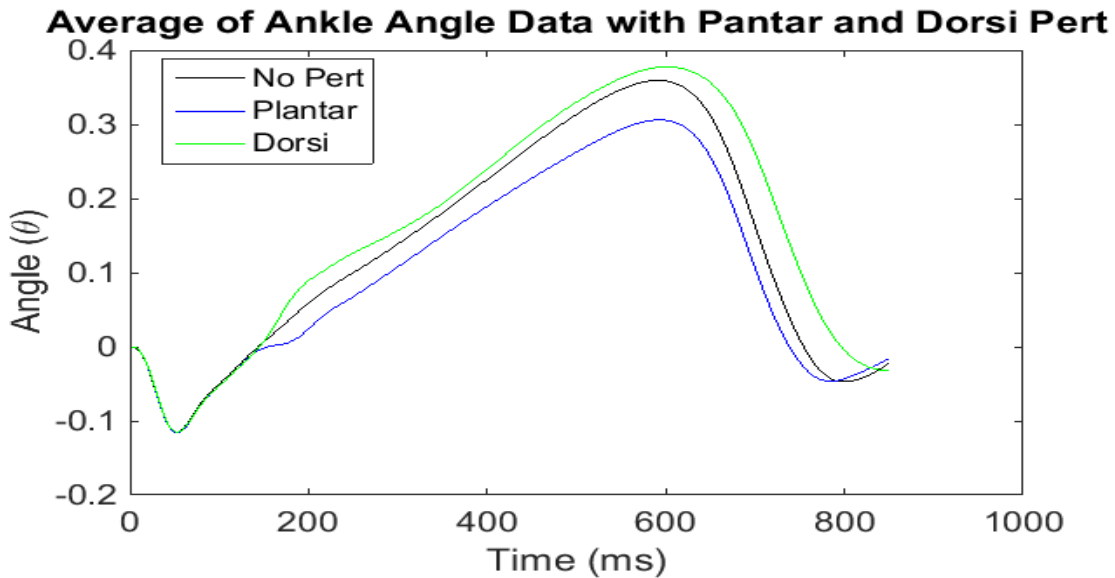


Figure 2.15: The normalized average of the ankle angle with no perturbation and also plantarflexive and dorsiflexive perturbation at 2° tilt of force plate and 100 ms perturbation.

the stance phase of gait. These small bumps are of importance in analysing the effect of perturbations on the ankle movement.

Here, in Fig. 2.19, the curve of the angle of the ankle dips down after the three points of the plantarflexive perturbation. This represents the plantarflexive direction of the perturbation. Each dip is right after the occurrence of the perturbation, and it is visible that the time point of the perturbation changes the magnitude of the ankle angle at the maximum, which is the start of heel off in the gait. This visually signals that the data should be explored further. Calculations will be done to compare curves of the different perturbations.

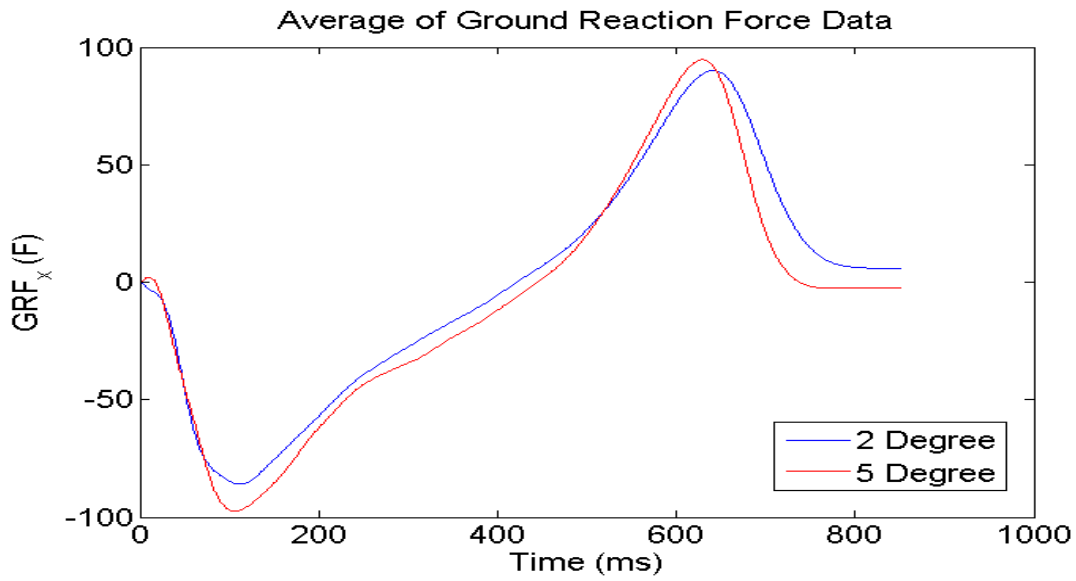


Figure 2.16: The average of ground reaction force in the x direction for all trials at 2° and 5° with no perturbation of a single subject.

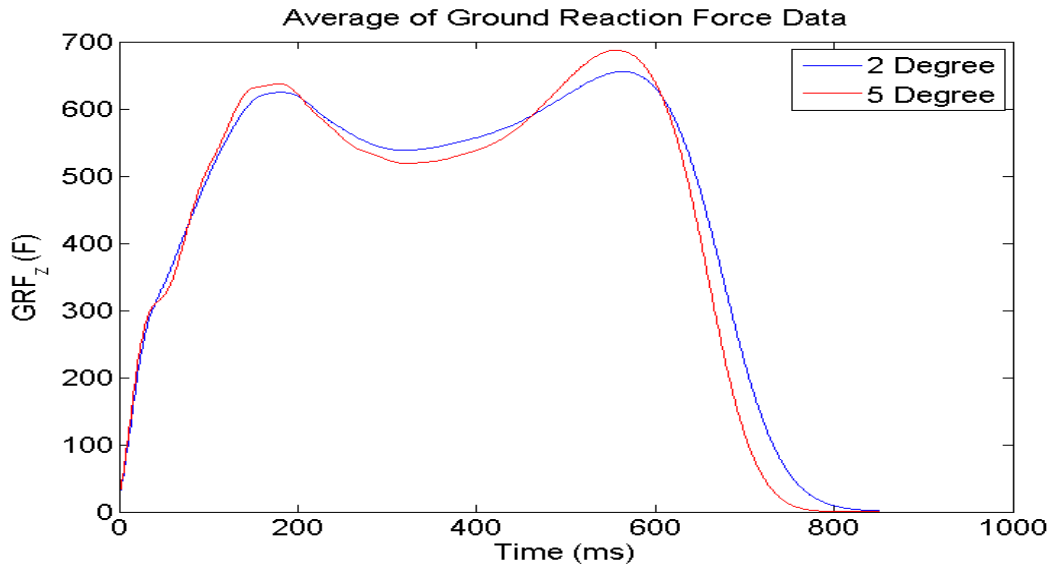


Figure 2.17: The average of ground reaction force in the z direction for all trials at 2° and 5° with no perturbation of a single subject.

In Fig. 2.20, the angle of the ankle never recovers back to its original curve, but instead it follows its pattern on an increased angle.

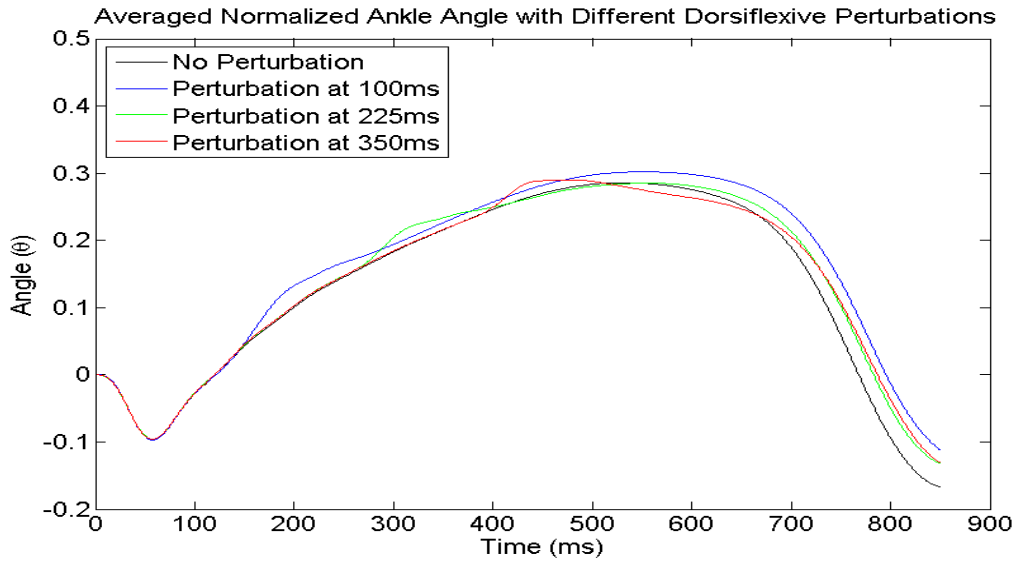


Figure 2.18: The average of normalized ankle angle with dorsiflexive perturbations that occurred at 100 ms, 225 ms, and 350 ms at the 2° tilt of force plate.

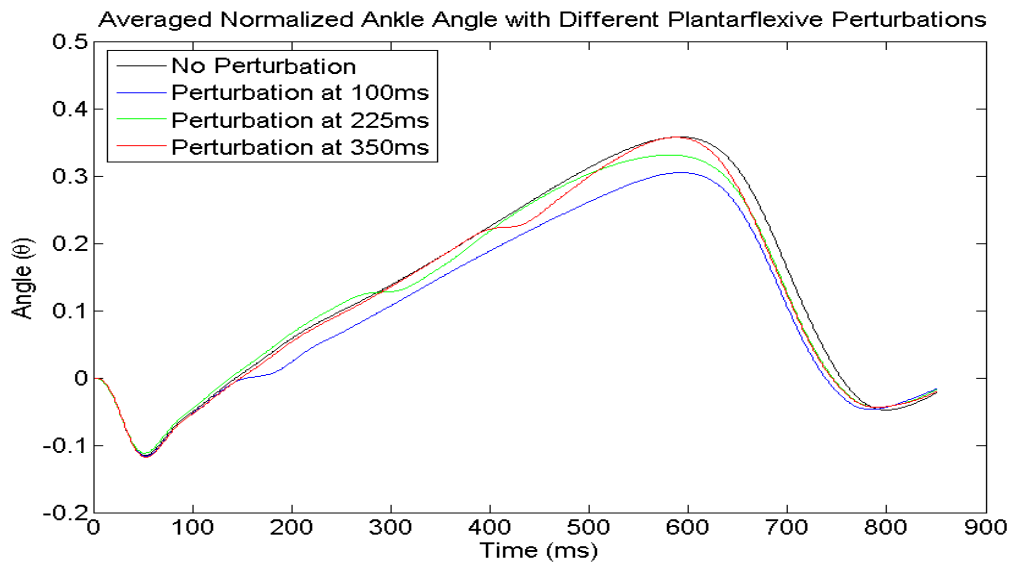


Figure 2.19: The average of normalized ankle angle with plantarflexive perturbations that occurred at 100ms, 225ms, and 350ms at the 2° tilt of the force plate.

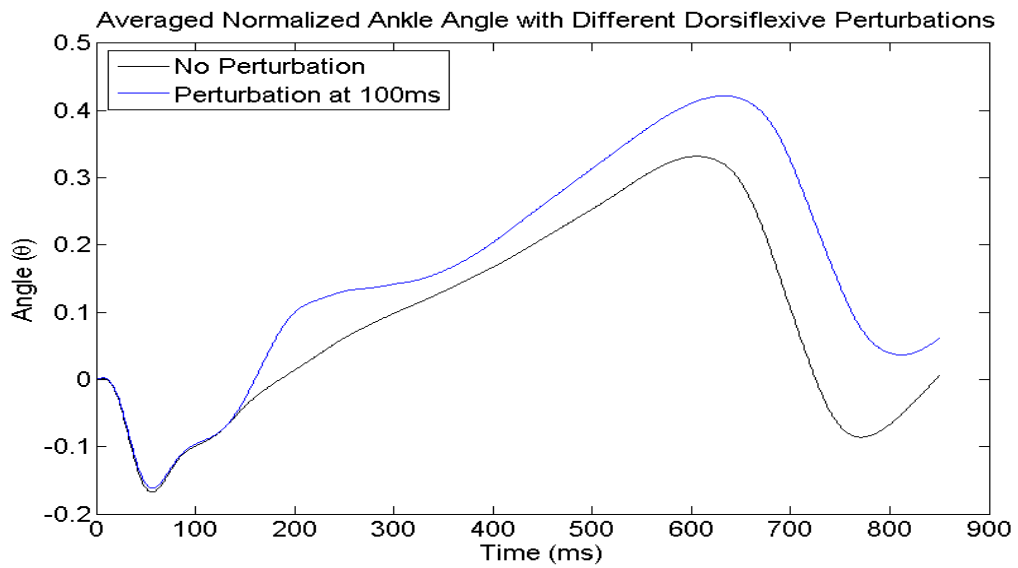


Figure 2.20: The average of normalized ankle angle with dorsiflexive perturbation that occurred at 100 ms at the 5° tilt of force plate.

Chapter 3

Analysis and Results

The goal of the study is to compare how the different perturbations affect the stance phase of the gait cycle. The analysis begins with the ankle data. At the sagittal plane, each cycle was analyzed by means of three peaks: foot flat (FF), midstance (M) and toe off (TO). The curves and analyzed peaks are shown in Fig. 2.13. The maximum (max) and minimum (min) values for the ankle motion during the gait cycle in the sagittal plane for one foot were calculated.

The study completed by Moriguchi suggests that a single individual's gait presents a regular pattern of movements, with little variation between cycles when the velocity is constant, but that individuals differ from each other [29]. Relatively low intra-individual variability was identified. However, the higher inter-individual variability found suggests that the ankle movement pattern can vary greatly, even among anthropometrically similar individuals. The analysis of our data will be done on a patient by patient basis [28]. There will be some discrepancies between the gait from subject to subject, and will be analysed separately. However, overall, the conclusion will cover all subjects.

3.1 Minimums and Maximums

Table 3.1 and Table 3.2 show minimums and the maximum of the 2° plantarflexive perturbation of ankle angle data. The first minimum occurs at the point of the subphase called foot flat with respect to the walk cycle. The maximum represents midstance of the walk. The second minimum occurs at toe off. These three subphases are crucial in the gait cycle. They explain the change in the slope of the angle of the ankle. They correspond with the curve of the ankle angle in the graphs in the previous section.

Similarly, Table 3.3 displays the minimums and the maximum for 5° plantarflexive perturbation of the ankle angle data. These peaks are characteristics of each individual subject's gait. The non-perturbed minimum and the minimums at each of the perturbations (100 ms, 225 ms, and 350 ms) can be compared to see any significance in the fluctuation of each subject's gait cycle.

The maximums of the ankle angle data are compared between the non-perturbed data and the perturbed data as well as the minimums. This can be referred back to stiffness. The maximum of the ankle angle in the plantarflexive position is the global maximum number of ankle angle. The minimum plantarflexion is the minimum value of the ankle angle data which is the global minimum of the ankle angle.

The range of motion for the human ankle is therefore the sum of maximum and absolute value of the

Table 3.1: The minimums and maximum of normalized ankle angle with plantarflexive perturbations at 2° tilt of the force plate.

Subject	Perturbation	Minimum 1 (time)	Maximum (time)	Minimum 2 (time)
Subject AB22	No Pert	-0.1242 (54 ms)	0.3759 (601 ms)	-0.2444 (829 ms)
	100ms Pert	-0.1233 (55 ms)	0.3812 (631 ms)	-0.1962 (821 ms)
	225ms Pert	-0.1306 (55 ms)	0.3728 (601 ms)	-0.2368 (831 ms)
	350ms Pert	-0.1252 (55 ms)	0.4095 (612 ms)	-0.1835 (821 ms)
Subject AB32	No Pert	-0.1314 (53 ms)	0.4050 (630 ms)	-0.1743 (838 ms)
	100ms Pert	-0.1331 (52 ms)	0.3739 (622 ms)	-0.1841 (824 ms)
	225ms Pert	-0.1312 (53 ms)	0.3597 (613 ms)	-0.2036 (826 ms)
	350ms Pert	0.1264 (52 ms)	0.3806 (619 ms)	-0.2008 (822 ms)
Subject AB34	No Pert	-0.1637 (57 ms)	0.3398 (641 ms)	-0.1794 (814 ms)
	100ms Pert	-0.1628 (57 ms)	0.2963 (639 ms)	-0.1942 (810 ms)
	225ms Pert	-0.1710 (58 ms)	0.3157 (635 ms)	-0.1546 (792–793 ms)
	350ms Pert	-0.1678 (58 ms)	0.3504 (628 ms)	-0.1921 (805 ms)
Subject AB43	No Pert	-0.1449 (52 ms)	0.4519 (623 ms)	-0.2467 (850 ms)
	100ms Pert	-0.1454 (51 ms)	0.4332 (625 ms)	-0.2904 (850 ms)
	225ms Pert	-0.1426 (52 ms)	0.4261 (637 ms)	-0.2932 (850 ms)
	350ms Pert	-0.1394 (52 ms)	0.4733 (624 ms)	-0.3230 (850 ms)
Subject AB93	No Pert	-0.0791 (59 ms)	0.1631 (581 ms)	-0.3979 (840 ms)
	100ms Pert	-0.0767 (59 ms)	0.1299 (581 ms)	-0.4031 (828 ms)
	225ms Pert	-0.0800 (59 ms)	0.1502 (581 ms)	-0.4107 (828 ms)
	350ms Pert	-0.0819 (59 ms)	.1932 (581 ms)	-0.3908 (832 ms)
Subject AB117	No Pert	-0.1573 (66 ms)	0.3325 (543 ms)	-0.2730 (803 ms)
	100ms Pert	-0.1647 (65 ms)	0.3010 (540 ms)	-0.3010 (796 ms)
	225ms Pert	-0.1676 (66 ms)	0.3016 (539 ms)	-0.2739 (796 ms)
	350ms Pert	-0.1722 (67 ms)	0.3171 (561 ms)	-0.2977 (801 ms)
Subject AB118	No Pert	-0.1148 (52 ms)	0.3591 (591 ms)	-0.0473 (799–800 ms)
	100ms Pert	-0.1162 (53 ms)	0.3059 (593 ms)	-0.0465 (783–786 ms)
	225ms Pert	-0.1118 (52 ms)	0.3322 (582 ms)	-0.0435 (791 ms)
	350ms Pert	-0.1177 (53 ms)	0.3585 (588 ms)	-0.0433 (790 ms)

minimum. This is useful in designing prosthetics. By analyzing the human gait cycle with the emphasis on the observations of how the ankle moves and the range of motion, it will contribute to making better orthopaedic devices such as prosthetics. Some references to the review papers are “Powered Ankle-Foot Prosthesis” [1] and “Kinematic and Dynamic Analysis of the Gait Cycle of Above-Knee Amputees” [14].

3.2 Correlation Coefficient Analysis

Correlation between sets of data is a measure of how well they are related [31]. The Table 3.4 shows the correlation coefficients for the ankle angle data at 2° plantarflexive perturbations. The most common measure of correlation is Pearson product–moment correlation coefficient, developed by Karl Pearson or simply correlation coefficient. It is a measure of the linear correlation or dependence between

Table 3.2: Continuation of the minimums and maximum of normalized ankle angle with plantarflexive perturbations at 2° tilt of the force plate.

Subject	Perturbation	Minimum 1 (time)	Maximum (time)	Minimum 2 (time)
Subject AB121	No Pert	-0.0961 (58 ms)	0.2860 (532 ms)	-0.1664 (850 ms)
	100ms Pert	-0.0939 (58 ms)	0.2541 (500 ms)	-0.1758 (833 ms)
	225ms Pert	-0.0999 (57 ms)	0.2658 (512 ms)	-0.1951 (835 ms)
	350ms Pert	-0.0956 (58 ms)	0.2893 (550 ms)	-0.1808 (834 ms)
Subject AB122	No Pert	-0.2091 (54 ms)	0.3172 (499 ms)	-0.3474 (790 ms)
	100ms Pert	-0.2071 (53 ms)	0.2745 (485 ms)	-0.3919 (773 ms)
	225ms Pert	-0.2087 (55 ms)	0.2954 (486 ms)	-0.4152 (778 ms)
	350ms Pert	-0.2024 (54 ms)	0.3330 (524 ms)	-0.3874 (794 ms)
Subject AB126	No Pert	-0.0965 (54 ms)	0.4057 (569 ms)	-0.0869 (832–835 ms)
	100ms Pert	-0.0970 (54 ms)	0.3751 (567 ms)	-0.1029 (824 ms)
	225ms Pert	-0.0937 (53 ms)	0.3925 (563 ms)	-0.0891 (818–821 ms)
	350ms Pert	-0.0920 (53 ms)	0.4047 (551 ms)	-0.0979 (823 ms)

Table 3.3: The minimums and maximum of normalized ankle angle with plantarflexive perturbations at 5° tilt of the force plate.

Subject	Perturbation	Minimum 1 (time)	Maximum (time)	Minimum 2 (time)
Subject AB53	No Pert	-0.2010 (64 ms)	0.0352 (610 ms)	-0.2066 (775 ms)
	100ms Pert	-0.2058 (64 ms)	-0.0433 (602 ms)	-0.2732 (759 ms)
Subject AB117	No Pert	-0.2319 (71 ms)	0.1346 (571 ms)	-0.1984 (836–839 ms)
	100ms Pert	-0.2335 (70 ms)	0.0470 (551 ms)	-0.2550 (815 ms)
Subject AB118	No Pert	-0.1678 (56 ms)	0.3319 (606 ms)	-0.0859 (770–772 ms)
	100ms Pert	-0.1711 (57 ms)	0.2339 (612 ms)	-0.1496 (764–765 ms)
Subject AB122	No Pert	-0.2175 (59 ms)	0.3577 (563 ms)	-0.2569 (777 ms)
	100ms Pert	-0.2239 (58 ms)	0.2674 (550 ms)	-0.2866 (767 ms)
Subject AB135	No Pert	-0.1087 (50 ms)	0.3467 (622 ms)	-0.2509 (838 ms)
	100ms Pert	-0.1082 (50 ms)	0.2541 (616 ms)	-0.2976 (822 ms)
Subject AB140	No Pert	-0.1785 (64 ms)	0.2429 (543 ms)	-0.4315 (778 ms)
	100ms Pert	-0.1740 (64 ms)	0.1477 (537 ms)	-0.4420 (742 ms)
Subject AB141	No Pert	-0.1107 (57 ms)	0.2426 (531 ms)	-0.3391 (758 ms)
	100ms Pert	-0.1167 (57 ms)	0.1748 (529 ms)	-0.3830 (744 ms)

two variables. It is widely used in the sciences as a measure of the degree of linear dependence between two variables. In other words, a Pearson product–moment correlation attempts to draw a line of best fit through the data of two variables, and correlation coefficient, R , indicates how far away all these data points are to this line of best fit.

It ranges between +1 and -1 inclusively. A value of 0 indicates that there is no association between the two variables. A value greater than 0 indicates a positive association, which means that as the value of one variable increases, so does the value of the other variable. A value less than 0 indicates a negative association. This means that as the value of one variable increases, the value of the other variable decreases. Values between +1 and -1 indicate that there is variation around the line of best fit. The closer the value of R is to 0, the greater the variation around the line of best fit.

Table 3.5 displays the correlation coefficients of the ankle angle data at 5° plantarflexive pertur-

Table 3.4: The correlation coefficient of normalized ankle angle with plantarflexive perturbations at 2° perturbation.

Subject	No Pert vs 100 ms Pert	No Pert vs 225 ms Pert	No Pert vs 350 ms Pert
Subject AB22	0.9426	0.9364	0.9229
Subject AB32	0.8824	0.8729	0.8687
Subject AB34	0.7758	0.7775	0.8384
Subject AB43	0.7535	0.7201	0.6892
Subject AB93	0.8751	0.8974	0.8890
Subject AB117	0.8543	0.8642	0.8518
Subject AB118	0.8075	0.8257	0.8136
Subject AB121	0.7735	0.7839	0.8178
Subject AB122	0.8782	0.8831	0.8769
Subject AB126	0.8708	0.8748	0.8617

bations. Statistically, the correlation coefficient of two variables in a data sample is their covariance divided by the product of their individual standard deviations. It is a normalized measurement of how the two are linearly related.

Formally, the sample correlation coefficient between two variables, x and y , is defined by the following formula, where s_x and s_y are the sample standard deviations for x sample and y sample respectfully, and s_{xy} is the sample covariance between the two [42].

$$r_{xy} = \frac{s_{xy}}{s_x s_y} \quad (3.1)$$

The covariance of two variables x and y in a data sample measures how the two are linearly related. A positive covariance would indicate a positive linear relationship between the variables, and a negative covariance would indicate the opposite. The sample covariance is defined in terms of the sample means as

$$s_{xy} = \frac{1}{n-1} \sum_{i=1}^n (x_i - \bar{x})(y_i - \bar{y}) \quad (3.2)$$

where n is sample size, x_i is a single value of x and y_i is a single value of y . The \bar{x} is the mean of all x samples and \bar{y} is the mean of all y samples. The mean is denoted by:

$$\bar{x} = \frac{\sum_{i=1}^n (x_i)}{n} \quad \text{and} \quad \bar{y} = \frac{\sum_{i=1}^n (y_i)}{n} \quad (3.3)$$

The standard deviation of an observation variable is the square root of its variance. The variance is a numerical measure of how the data values are dispersed around the mean. The sample variance is defined as

$$s_x^2 = \frac{1}{n-1} \sum_{i=1}^n (x_i - \bar{x})^2 \quad (3.4)$$

where n is sample size. The standard deviation is just the square root of Equation (3.4).

The numbers in Table 3.4 and Table 3.5 are calculated using the matlab *corrcoef*(X, Y) function [12], which is related to the covariance matrix *cov*(X) [13]. It takes in two column vectors of non perturbed data and the perturbed data, and it then produces the correlation coefficient.

Table 3.5: The correlation coefficient of normalized ankle angle with plantarflexive perturbations at 5° perturbation.

Subject	No Pert vs 100 ms Pert
Subject AB53	0.6519
Subject AB117	0.8140
Subject AB118	0.9117
Subject AB122	0.8912
Subject AB135	0.8980
Subject AB140	0.7469
Subject AB141	0.9036

Since most of the correlation coefficients were approximately close to 1, we can conclude that the variables that were compared are positively linearly related. This suggested a fairly strong relationship. The non-perturbed and the perturbed data of the ankle angle follow the same trend. The graph such as in Figure 2.19 of the previous section shows how both curves decrease, then increase and slightly decrease at the end. The high R represents that even though the perturbations occurred, this does not deter the subject from their normal gait pattern, the subjects were still able to follow the same pattern and trend of their walk.

3.3 T-Test Analysis

A t-test is any statistical hypothesis test in which the test statistic follows a Student's t distribution. It can be used to determine if two sets of data are significantly different from each other. A paired t-test is used to compare two population means where observations in one sample can be paired with observations in the other sample. A paired t-test looks at the difference between paired values in two samples, takes into account the variation of values within each sample, and produces a single number known as a t-value. The equation of a t-test is:

$$t = \frac{\bar{d}}{\sqrt{\frac{s^2}{n}}} \quad (3.5)$$

where \bar{d} is the mean difference between the two samples, s^2 is the sample variance, n is the sample size, and t is a paired sample t-test with $n-1$ degrees of freedom [31].

The assumptions for a paired t-test: Each of the two populations being compared should follow a normal distribution with $\mathcal{N} \sim (\mu, \sigma)$, which means the mean is μ and standard deviation is σ . The two populations being compared should have the same variance, σ^2 . The equation of a normal distribution is Equation (3.7). If the sample sizes in the two groups being compared are equal, the t-test is highly robust to the presence of unequal variances. The last assumption is that the data used to carry out the test should be sampled independently from the two populations being compared.

The null hypothesis is that the pairwise difference between data vectors x and y has a mean equal to zero. The MATLAB `ttest(x,y)` function [9] returns a test decision for the null hypothesis that the data in $x-y$ comes from a normal distribution with mean equal to zero and unknown variance, using the paired-sample t-test.

We were running a paired t-test. This t-test compares one set of measurements with a second

set from the same sample. The averaged ankle angle data with no perturbation is compared with the averaged ankle angle data with each level of perturbation (100ms, 225ms, 350ms) for each subject at both 2° and 5°.

The non-perturbed data is compared with each of the perturbation data and extremely small t-values are produced. We have to reject the null hypothesis, and thus, the results are statistically significant. The ankle angle data set is checked to see if it satisfies a normal distribution. It already has equal sample sizes in the two groups, and it is sampled independently.

The function $kstest(X)$ in MatLab [8] is used to check the data of the ankle angle for the normal distribution. This function returns a test decision for the null hypothesis that the data in vector X comes from a standard normal distribution, against the alternative that it does not come from such a distribution, using the one-sample Kolmogorov-Smirnov test. The result h is 1 if the test rejects the null hypothesis at the 5% significance level, or 0 otherwise.

The general formula for the probability density function of the normal distribution with mean, μ , and variance, σ^2 , is

$$f(x) = \frac{1}{\sigma\sqrt{2\pi}} e^{-(x-\mu)^2/(2\sigma^2)} \quad (3.6)$$

The case where $\mu = 0$ and $\sigma = 1$ is called the standard normal distribution [31]. The equation for the standard normal distribution is

$$f(x) = \frac{e^{-x^2/2}}{\sqrt{2\pi}} \quad (3.7)$$

The Kolmogorov-Smirnov Test is a goodness-of-fit test for any statistical distribution. The test relies on the fact that the value of the sample cumulative density function is asymptotically normally distributed. To apply the Kolmogorov-Smirnov test, the cumulative frequency (normalized by the sample size) of the observations is calculated. Then the cumulative frequency for a true distribution (most commonly, the normal distribution) is calculated. Then one would need to find the greatest discrepancy between the observed and expected cumulative frequencies, which is called the “D-statistic”, and then compare this against the critical D-statistic for that sample size. If the calculated D-statistic is greater than the critical one, then reject the null hypothesis, which is the distribution of the expected form [41]. The Kolmogorov-Smirnov test statistic:

$$D_n = \sup_x [|F_n(x) - F_0(x)|] \quad (3.8)$$

is used for testing the null hypothesis that the cumulative distribution function $F(x)$ equals some hypothesized distribution function F_0 , that is, $H_0 : F(x) = F_0(x)$, against all of the possible alternative hypotheses $H_A : F(x) \neq F_0(x)$. That is, D_n is the least upper bound of all pointwise differences $|F_n(x) - F_0(x)|$.

After running the $kstest(X)$ on the ankle angle that that was averaged over all the trials for each subject, the result was $h = 1$. Therefore, the data does not have a standard normal distribution, and the t-test will not yield reasonable results. Also the same conclusion happened when the vector of minimums and the vector of maximums were checked for the normal distributions. Both data sets do not have normal distributions.

To again check the normality of the data sets. The MATLAB function $histfit$ is used [11]. $histfit(data, nbins)$ plots a histogram using n bins and fits a normal density function. Figure 3.1 shows the histogram of the maximums that occurred at all trials for subject AB126 at 100 ms plantarflexive perturbation. The maximums were grouped into 10 bins and put on a normal distribution. However, the data does not reflect normality. The maximums are uneven and do not follow the red normal curve.

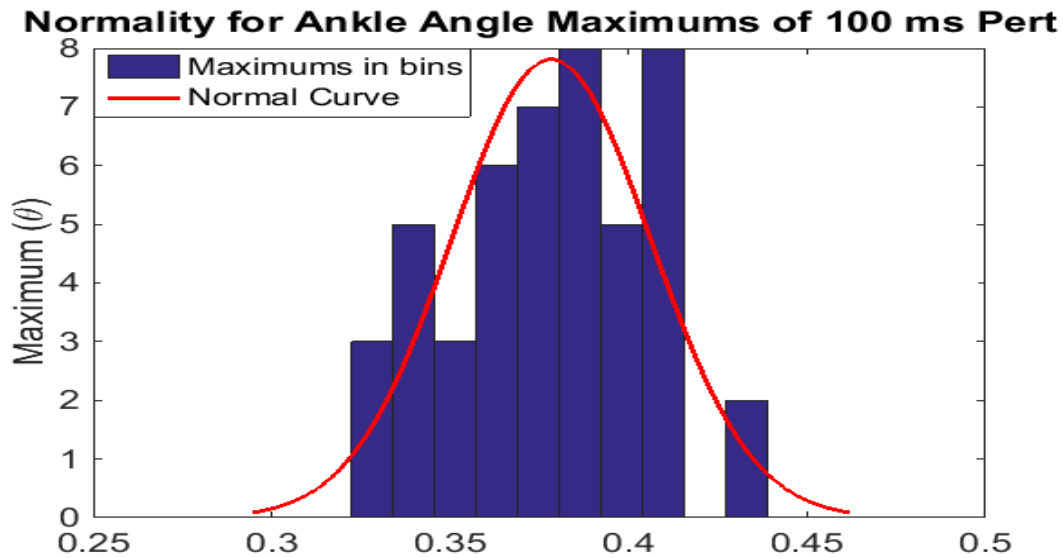


Figure 3.1: The normality test using a histogram of values in data to fit a normal density function for Subject AB126 for 2° 100 ms plantarflexive perturbation.

3.4 Passing–Bablok Regression

Additionally, Passing–Bablok Regression was used to give additional insight to the perturbed and non-perturbed data. Passing and Bablok developed a regression method that allows comparing two measurement methods, which overcomes the assumptions of the classical linear regression. Passing–Bablok compares two analytical methods, a test method against a reference or comparative method, to determine analytical accuracy [18].

The requirements of the test are that two methods are measured continuously, and any number of replicates can be observed for each method, though all cases must have the same number of replicates. The report shows the number of cases analyzed. Constant and proportional bias are shown after. When two methods produce equivalent results, the constant bias will be zero and proportional bias will be one. Confidence intervals show the range that likely contains the true constant and proportional bias. The scatter plot shows the observations of reference method (X) plotted against the test method (Y). After the scatter plot is a residual plot of the difference of test method from the fit. A CUSUM linearity test determines if the residuals are randomly distributed around the fitted line. A significant p-value indicates the method is non-linear.

Figure 3.2 shows the Passing–Bablok regression fit. The Passing–Bablok’s method for assessing the equality of measurements uses two different analytical methods. The x-axis is the comparative method (A), y-axis is the test method (B), and the line of equality ($y=x$) is the red dashed line. Passing–Bablok compares the two methods. Both axes extend from 0 to the highest result. It is fitting unbiased linear regression line to data in the method of comparing studies. It calculates the unbiased slope and intercept, along with their confidence intervals. It does not matter which results are assigned to “method A” and “method B”. However, “method A” results will be plotted on the x-axis by the *plot* method. In the graph, the method B is the x-axis and method A is the y-axis. The circular dots are the observations, the red line is the line of equality between methods, the blue solid line is the fitted regression line, and the black dashed lines are the regression line confidence bands.

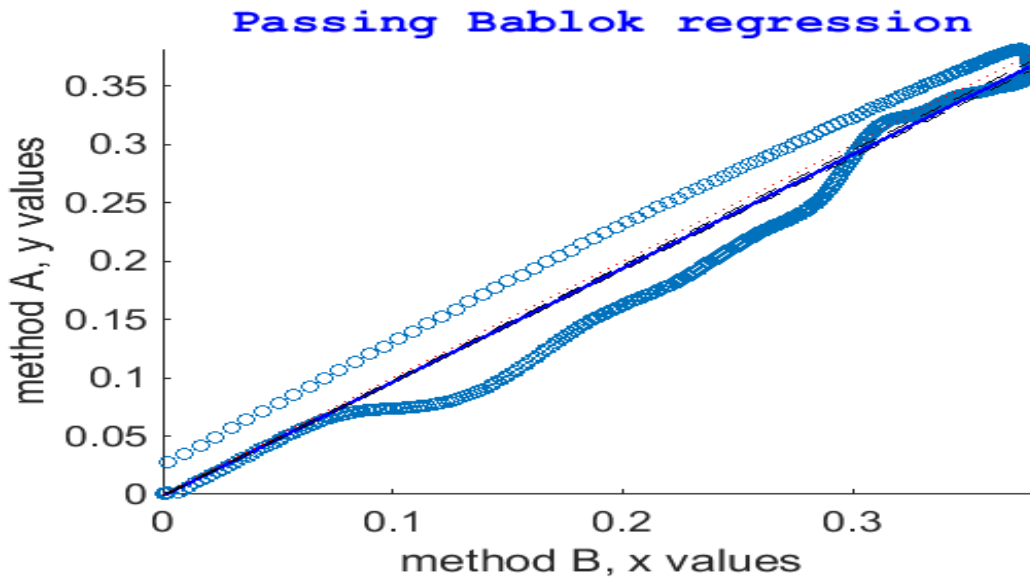


Figure 3.2: PassingBablok regression fit for ankle angle averages of Subject AB22 at 2 degrees for no perturbation and 100 ms plantarflexive perturbation.

Figure 3.3 shows the Passing–Bablok ranked residual plot. A residual is the difference between the observed y -value from scatter plot and the predicted y -value from regression equation line. It is the vertical distance from the actual plotted point to the point on the regression line. It is also how far the data falls from the regression line. Below is a residual plot of the difference of test methods from the fit. The red straight line is the zero/fitted regression line. The circular dots are the residual of each observation, which again is differences of the observed from the fitted line [18].

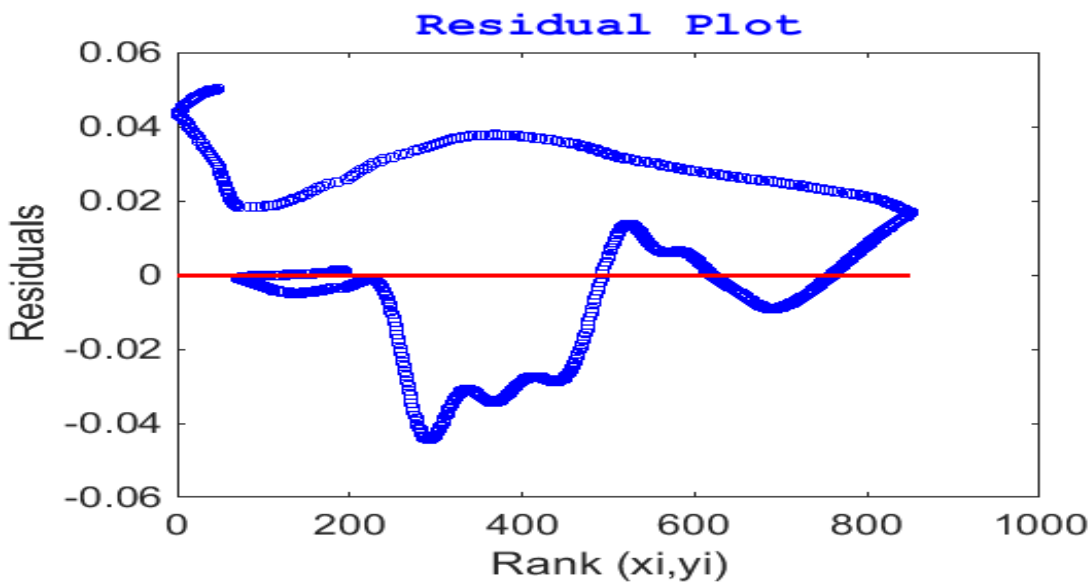


Figure 3.3: PassingBablok ranked residual plot for ankle angle averages of Subject AB22 for perturbed and 100 ms plantarflexive perturbation.

Figure 3.4 shows the Passing–Bablok linearity of tests plot. A CUSUM plot and CUSUM linearity

test can be shown to help judge the linearity of the method. A CUSUM linearity test determines if the residuals are randomly distributed around the fitted line. A significant p-value indicates the method is non-linear. The linearity plot visually shows the running total of the number of observations above the fitted line, which are counted as +1 and below the fitted line, which are counted as -1. Ideally, there should be roughly equal numbers of observations above and below the zero line, with the line roughly about zero. If clusters of observations form on either side of the zero line the method may be non-linear. The measurement number of observations are the Rank(xi, yi), where i is the index of each pair of the two methods. It is also the number of points in each method. The CUMSUM shows where each observation lies within the fitted line [18].

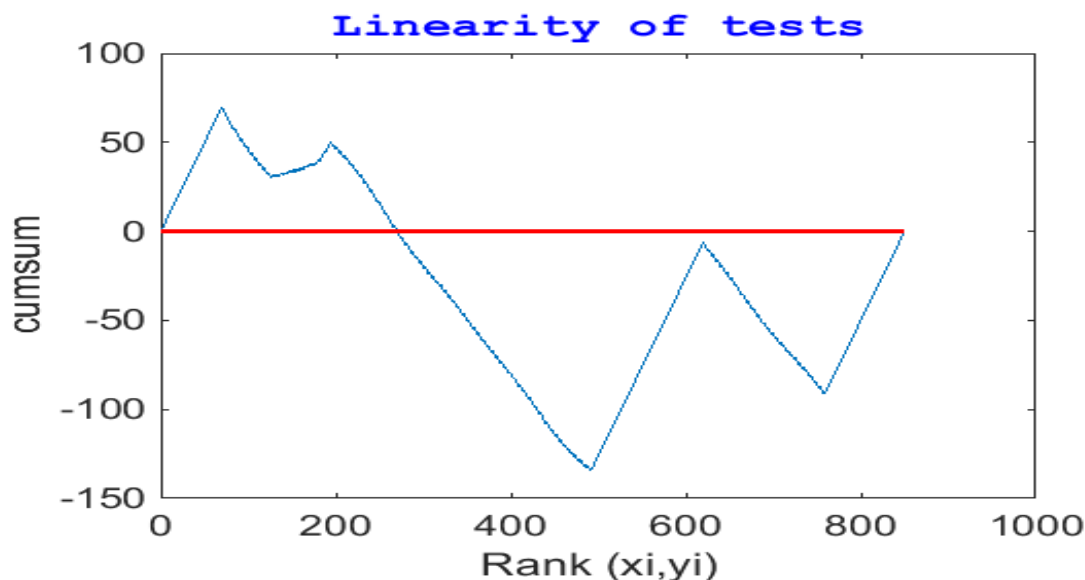


Figure 3.4: PassingBablok linearity test for ankle angle averages of Subject AB22 for no perturbation and 100 ms plantarflexive perturbation.

However, with our data, the test for linearity has failed. The linear relationship between no perturbation ankle angle data and perturbed ankle angle data is rejected. Non linear samples are not suitable for concluding on method agreement. We cannot conclude anything else from this test.

3.5 Ankle Angle Maximums Analysis

After gathering the minimums and maximums in the previous section, the maximums will be further analyzed. As mentioned before, the data starts at the point where the heel makes contact with the force plate. The first minimum occurs at the beginning of minstance, when the the toes touch the ground. The maximum occurs after midstance is completed. It is at heel off stage of the gait cycle. The data ends at toe off when the foot completely disconnects with the platform.

The first minimum is consistent throughout perturbed and non-perturbed data. The perturbations that occur during the midstance subphase and are after the first minimum, therefore analyzing the minimums will not give any information as to how the perturbations effect the walk cycle. This leaves the maximums. Thus, the different perturbed maximums of each subject are analyzed.

For subject AB126, the following ankle angle data produces the following maximums. No perturbation maximum is at 0.4057 angle, 100 ms perturbation maximum is at 0.3751 angle, 225 ms perturbation maximum is at 0.3925 angle and 350 ms perturbation maximum is at 0.4047 angle.

Figure 3.5 displays in a graph the maximums at no perturbation and then at each of the plantarflexive perturbations at 2°.



Figure 3.5: The maximums in order of occurrence of Subject AB121 for no perturbation and the 2° plantarflexive perturbations at 100 ms, 225 ms, and 350 ms.

The order in Figure 3.5 is the the order in which the perturbations occurred. Order 1 corresponds to non-perturbed maximum, order 2 is the maximum at 100 ms perturbation, order 3 is the maximum at 225 ms perturbation, order 4 is the maximum at 350 ms perturbation. Notice how the maximums change. The first maximum is the nominal maximum, which is used as a base line. There is a trend of the maximums with the perturbations to approach the nominal maximum as the perturbations increase.

Figure 3.6 is a different way of looking at the comparison of the maximums at the different plantarflexive perturbations.

The red dot is the nominal maximum (maximum at the non perturbation walk). The black dot is the maximum of the 100 ms plantarflexive perturbation at 2°. The blue dot is the maximum of the 225 ms perturbation, and the blue dot is the maximum of the 350 ms perturbation. The different lines represent the slopes between the non-perturbed maximum and each of the perturbations. Again, there is a drastic change in the maximums between no perturbation and 100 ms perturbation. Then the change in maximums decreases for 225 ms perturbation, and finally close to the nominal maximum for the 350 ms perturbation.

This signifies that the earliest perturbation has a much greater affect on the maximums of the ankle angle than the later occurring perturbations. Since the maximum is the beginning point of the heel off subphase of the gait, we are comparing the ankle angle degree that occurs at heel off. This shows that perturbations that occur early affect the magnitude of the ankle angle degree more. The perturbations occur at equidistant time intervals. However, the change in ankle angle is not equal from perturbation to perturbation.

Figure 3.7 shows the three slopes and how the magnitude of those slopes change. Notice that in Figure 3.7 the values of the slopes between the perturbations are the red stars, and the blue lines signify

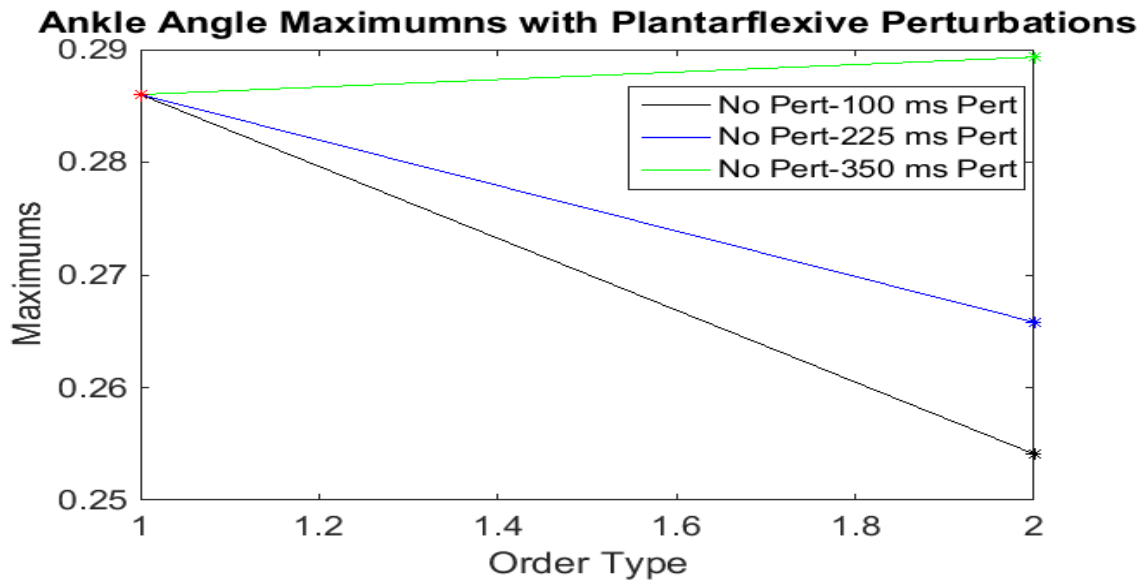


Figure 3.6: The maximum of Subject AB121 for no perturbation compared against the 2° plantarflexive perturbations maximums at 100 ms, 225 ms, and 350 ms.

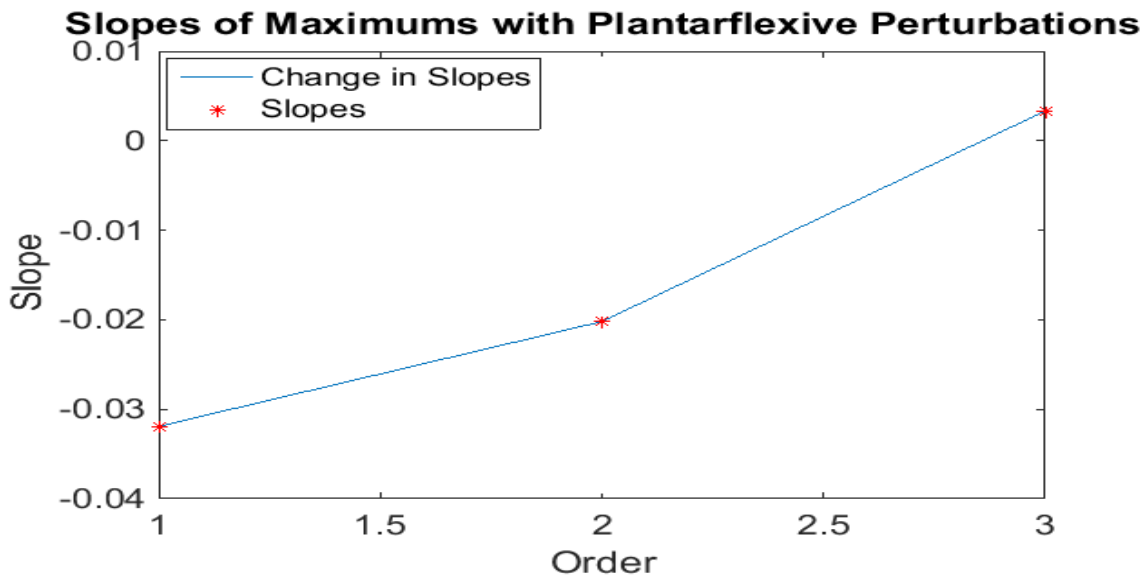


Figure 3.7: The slopes of the maximums of Subject AB121 for no perturbation and 2° plantarflexive perturbations at 100 ms, 225 ms, and 350 ms.

the increase from slope to slope. This shows that the slopes of the maximums have a steady increase. The last slope is close to zero, which means that the difference between non-perturbed nominal data and the data with the perturbation at 350 ms is practically zero. So if these maximums are very close in value, it results in the fact that the 350 ms perturbation has little effect on the maximum, which is the point at the end of midstance and beginning of heel off. The foot stabilizes quickly during the later perturbation. Whereas, the the slope significantly changes on the earlier perturbations.

Running the same test for other subjects gives the following results. Each subject has its unique pattern of recovery and should not be compared to other subjects, but rather the comparison goes

within each subject's different perturbations.

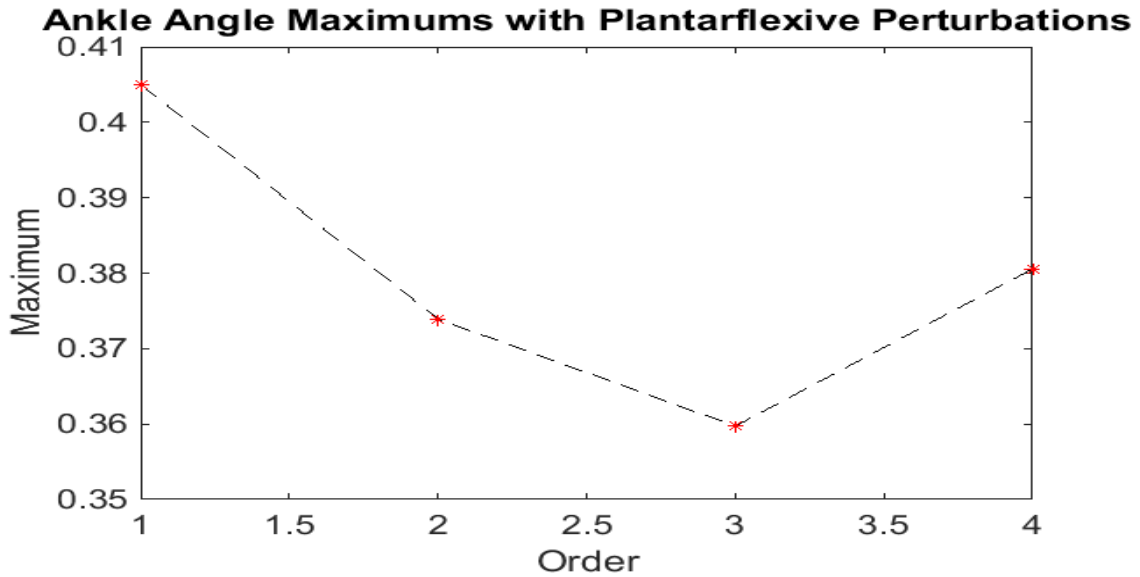


Figure 3.8: The maximums in order of occurrence of Subject AB32 for no perturbation and the 2° plantarflexive perturbations at 100 ms, 225 ms, and 350 ms.



Figure 3.9: The maximum of Subject AB32 for no perturbation compared against the 2° plantarflexive perturbations maximums at 100 ms, 225 ms, and 350 ms.

Figure 3.8 shows the maximums in order of occurrence of Subject AB32. Figure 3.9 shows the maximum of no perturbation compared to the maximums at the different perturbations of Subject AB32. Figure 3.10 shows the slopes of the maximums of the subject AB32.

For subject AB32, in Fig. 3.8-3.10, there is an even change between the maximums of the ankle angle. Due to each perturbation, the maximums adjust to follow the trend of the nominal gait, however it results in shifts of the perturbed curves. There is a decrease in the maximums that as the

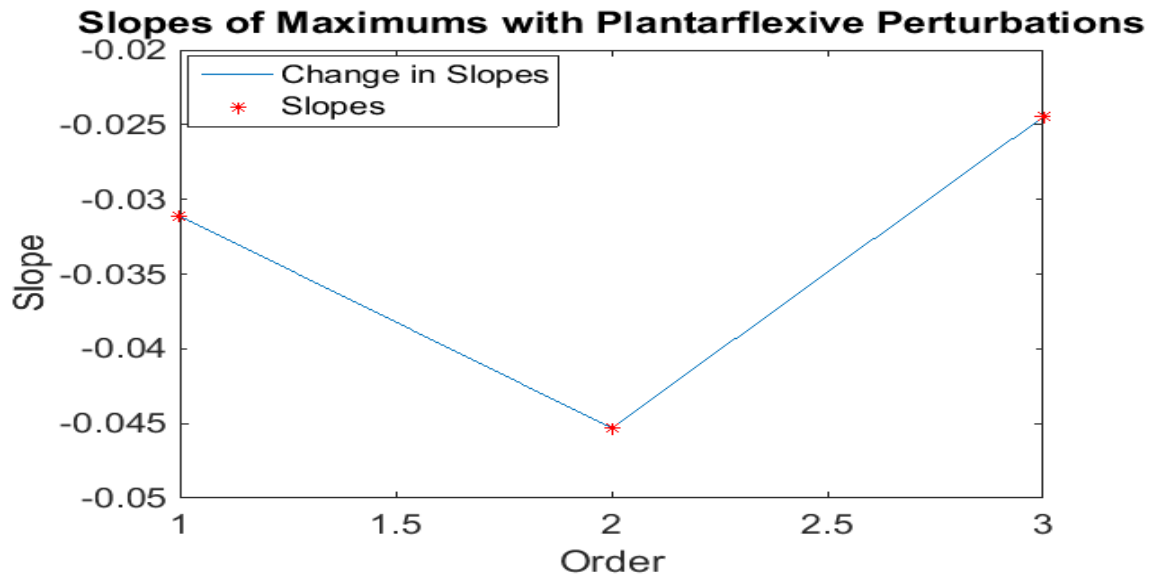


Figure 3.10: The slopes of the maximums of Subject AB32 for no perturbation and 2° plantarflexive perturbations at 100 ms, 225 ms, and 350 ms.

perturbations increase the pattern shifts more and more, until the last 350 ms perturbation where it aligns closer to the original curve.

Figure 3.11 shows the maximums in order of occurrence of Subject AB117. Here, there is also the significant change in the maximum for the earliest perturbation as well as the second. Then the 350 ms perturbation shows a closer value to the nominal maximum. This confirms that reaction of the perturbations is more drastic when the perturbations occur early.

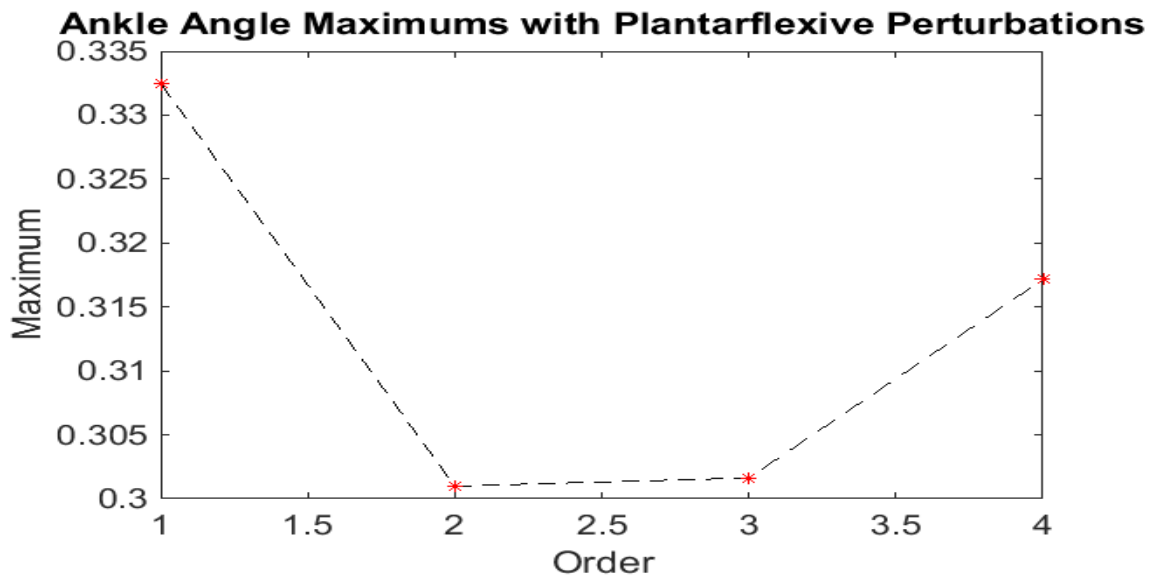


Figure 3.11: The maximums in order of occurrence of Subject AB117 for no perturbation and the 2° plantarflexive perturbations at 100 ms, 225 ms, and 350 ms.

Figure 3.12 shows the maximum of no perturbation compared to the maximums at the different

perturbations of Subject AB117. This had a good visual representation of how close the 100 ms and 225 ms maximums are and then how the 350 ms maximum is shifted up.

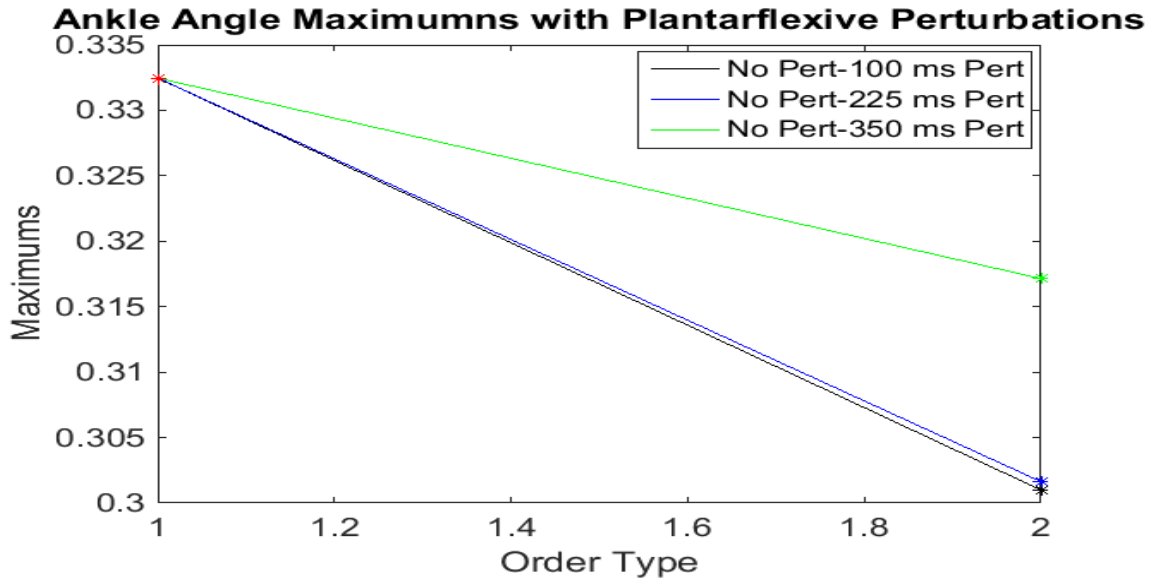


Figure 3.12: The maximum of Subject AB117 for no perturbation compared against the 2° plantarflexive perturbations maximums at 100 ms, 225 ms, and 350 ms.

Figure 3.13 shows the slopes of the maximums of the subject AB117. Looking at the slopes of the maximums, there is a gradual increase as the order increase, which means that the perturbations occur later in the stance phase.

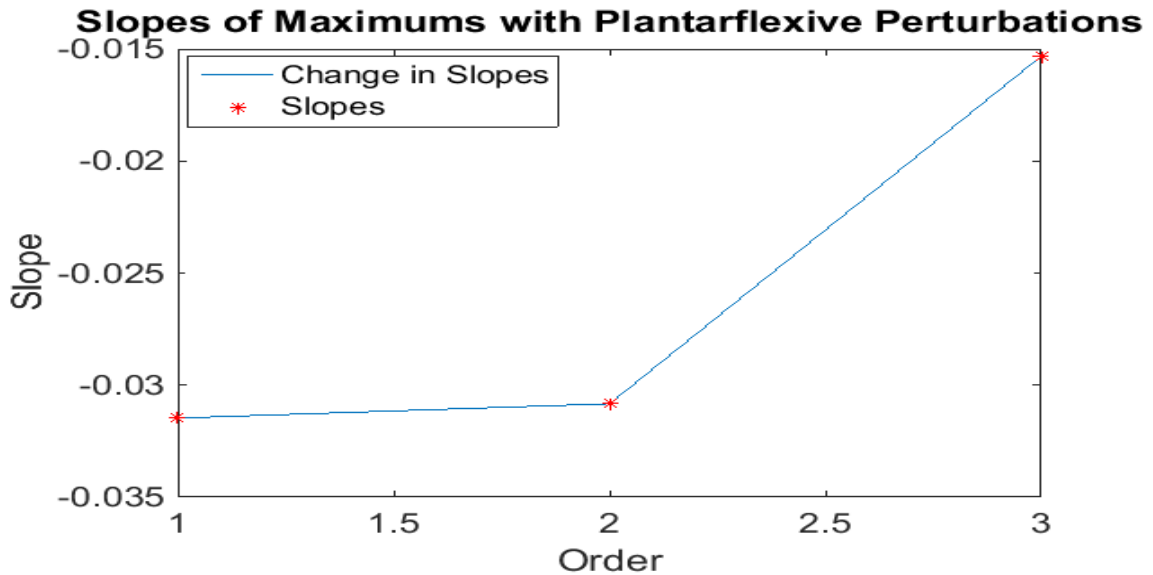


Figure 3.13: The slopes of the maximums of Subject AB117 for no perturbation and 2° plantarflexive perturbations at 100 ms, 225 ms, and 350 ms.

For subject AB117, notice how the first two maximums which are the 100 ms and the 225 ms perturbations are very similar in value, and then the 350 ms perturbation is closer to the nominal.

Again this shows that the further the perturbation happens in the stance phase the closer it returns to the non-perturbed values of the walk.



Figure 3.14: The maximums in order of occurrence of Subject AB43 for no perturbation and the 2° plantarflexive perturbations at 100 ms, 225 ms, and 350 ms.

Figure 3.14 shows the maximums in order of occurrence of Subject AB43. Figure 3.15 shows the maximum of no perturbation compared to the maximums at the different perturbations of Subject AB43. For this subject the maximums followed slightly a different trend but overall agree with the general idea. The maximum that occurred at the 225 ms perturbation is actually the smallest instead of the 100 ms perturbation maximum. However, the 350 ms perturbation is still significantly closer to the nominal maximum.

Figure 3.16 shows the slopes of the maximums of the subject AB43. This shows the characteristics of the maximums and how they are behaving as the perturbations increase. For subject AB43, notice how the maximums of ankle angle data gradually decrease and increase for the last one. For this, the closest value of the maximum to the non-perturbed maximum is actually the one that occurs at the 100 ms perturbation. It then continues to decrease and move away from the pattern of trend until it overshoots on the 350 ms perturbation and the slope of that pair of maximums is actually positive.

These several patients demonstrate that the perturbation that occurs at 225 ms is the least likely to adjust to the pattern of no perturbation from looking at the maximums of the curves. These maximums signify a distinct change in characteristic of gait where the mid-stance ends and heel-off begins.

3.6 COP Analysis

Another set of data that was gathered from the experiment was the center of pressure of the stance foot, (COP). As mentioned in Section 2.3, COP is the point of application of the ground reaction force vector. Also, it is the point of location of the vertical ground reaction force vector. Figure 3.17 shows the COP data of one of the subjects that walked across the force platform. Notice how after each perturbation, the center of pressure of the foot fluctuates as the foot tries to regain normal gait.

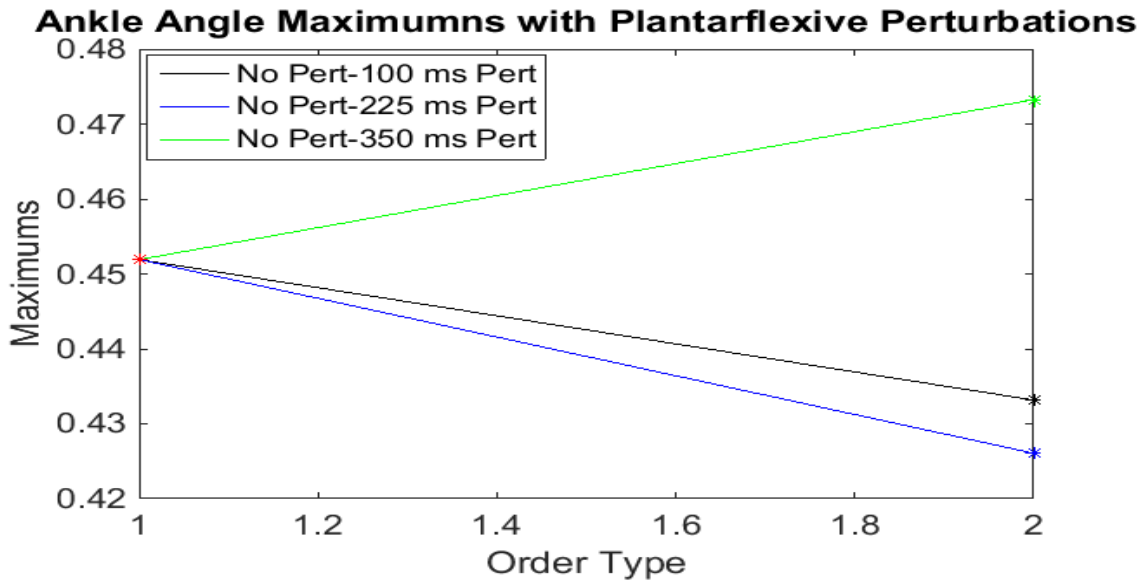


Figure 3.15: The maximum of Subject AB43 for no perturbation compared against the 2° plantarflexive perturbations maximums at 100 ms, 225 ms, and 350 ms.

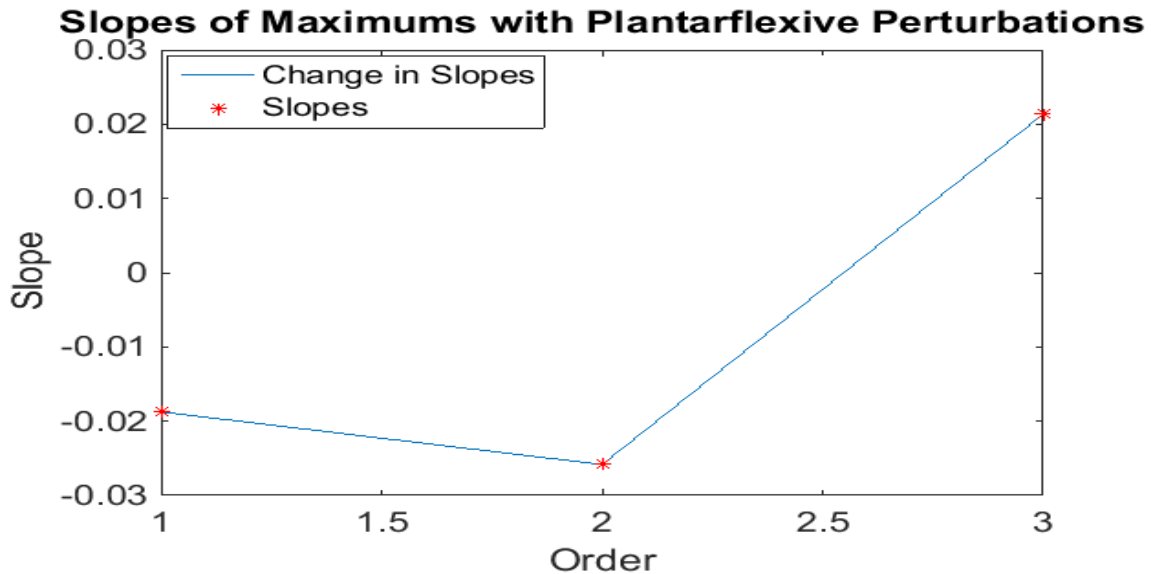


Figure 3.16: The slopes of the maximums of Subject AB43 for no perturbation and 2° plantarflexive perturbations at 100 ms, 225 ms, and 350 ms.

The fluctuation occurs for approximately 150 ms after each of the perturbations. Then, the center of pressure levels off and proceeds to exactly follow the center of pressure curve that was not perturbed.

During the stance phase, the center of pressure starts at the medial heel. As foot flat occurs and the body progresses to single stance, the center of pressure typically moves laterally as it progresses forward. Then after heel rise and the weight shifts, the center of pressure is in the forefoot progressing to the medial side again [7]. The COP data ranges from 0–850 ms. However, there was vast oscillations after 725 ms. This is due to the foot coming off the platform. The toes are losing contact and there is no accurate center of pressure at that point. It was necessary to reduce our analysis to only 0–700 ms.

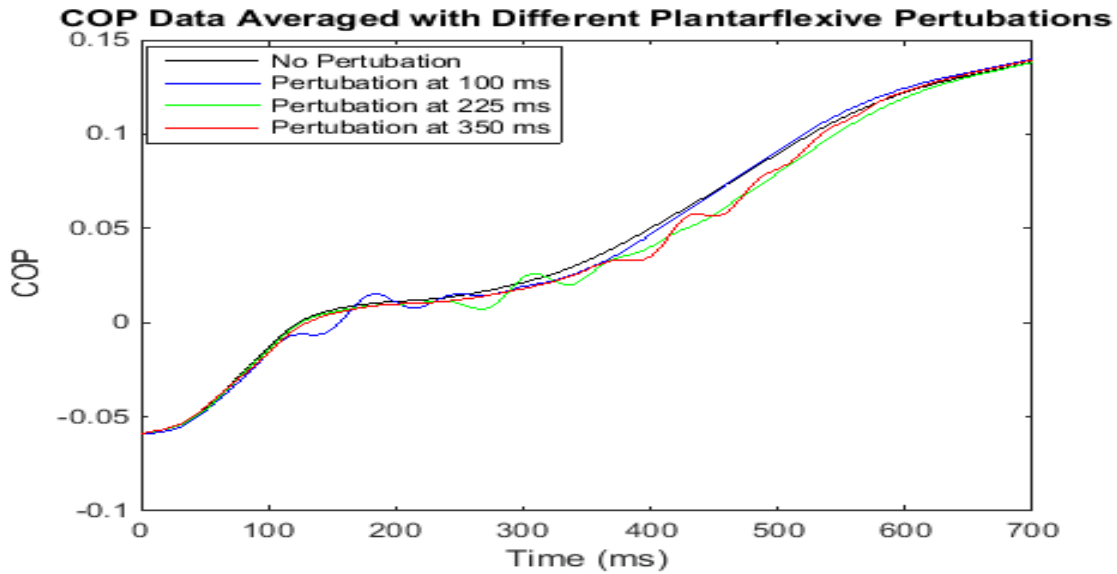


Figure 3.17: Center of pressure averaged over trials for subject AB43 with various perturbations at 2° tilt of force plate.

In Figure 3.18, there are both types of perturbations. The changes in the gait due to the perturbations are reflected in the change in center of pressure. During the walk, the center of pressure is near the heel at the time of heelstrike and moves throughout the step. It is located near the toes at toe-off. The force plate gathered data in the anterior-posterior direction (on the x -axis), which is forward and backward motion. The COP measurement is distance from the ankle angle of rotation to the center of pressure point on floor in the x direction. The ankle point of rotation has COP 0 because it is directly above. The negative COP represents the distance between heel and the ankle point of rotation. Positive COP is the measurement between the ankle center of rotation and toes.

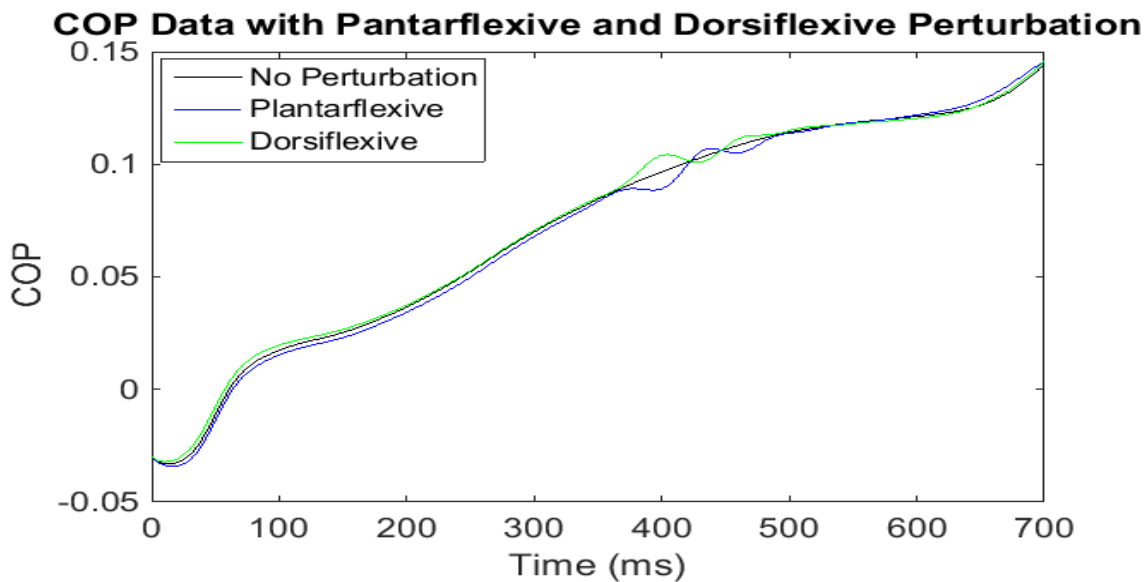


Figure 3.18: Center of pressure averaged over trials for subject AB118 with plantarflexive and dorsiflexive perturbations at 350 ms and 2°

The plantarflexive perturbation of the COP is the blue curve; it dips down and starts fluctuating at 350 ms. Then it is able to match with the non-perturbed COP curve. Similarly, the dorsiflexive perturbation of the COP is the green curve; it rises up and starts fluctuating also at 350 ms. It is able to match with the non-perturbed COP curve as well.

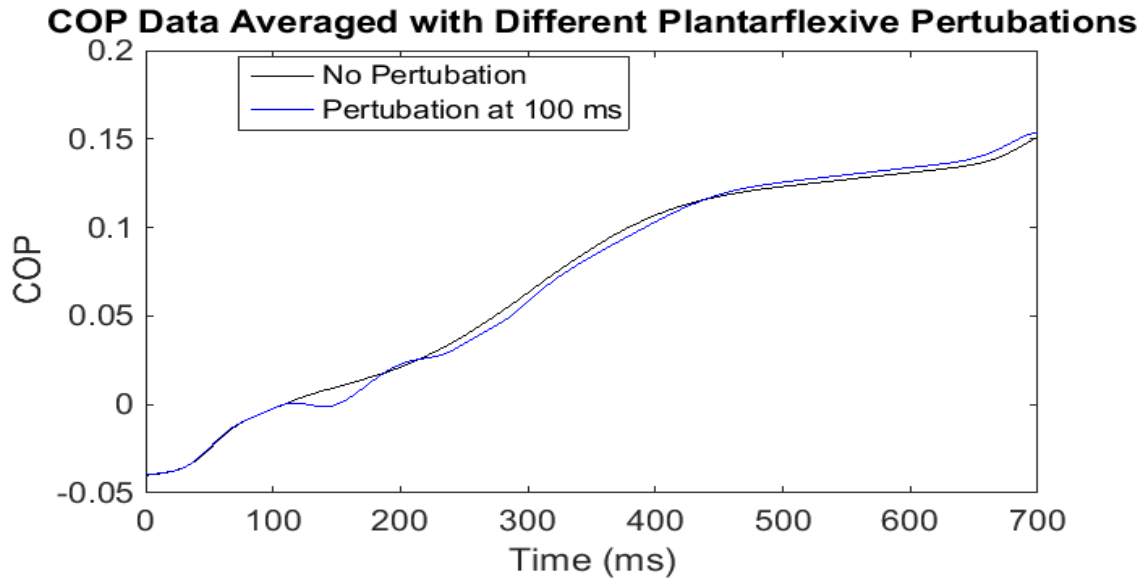


Figure 3.19: Center of pressure averaged over trials for subject AB122 with various perturbations at 5° tilt of the force plate.

Figure 3.19 is showing center of pressure at 5° perturbations that occurred at the different time-points. The change in the curve is more drastic due to the increase in force plate angle from 2° to 5°. This is expected since for the 5° perturbations, the force plate tilts more, resulting on more change in the gait. This is reflected in a bigger dip in the COP curve. The center of pressure had to shift more to accommodate for a sudden change in ground.

Figure 3.20 displays COP with both plantarflexive and dorsiflexive perturbations at 5° and 100 ms perturbation. This is a similar graph, however, notice how the plantarflexive and dorsiflexive perturbations are symmetric about the nominal curve. The gait is affected similarly for both types with the only difference being the direction of the dip in the graph.

The interesting aspect of these graphs is that the center of pressure is able to return to the exact same pattern as the center of pressure that did not under go any perturbation. The oscillatory effect only occurs locally within 150 ms of the occurring perturbation time. This means that, overall, the perturbations have no effect on center of pressure. Whereas, for the ankle angle data, the angle shifts its curve to account for the occurrence of the perturbation. It still follows its normal trend but not to the exact non-perturbed curve. In most cases, the ankle angle after perturbation is not able to return to the non-perturbed pattern. This is especially evident in 350 ms perturbations and in 5° data.

COP is related to balance. It is dependent on the position of the body with respect to the supporting surface. Center of pressure is the location on the supporting surface where the resultant vertical force vector would act if it could be considered to have a single point of application. A shift of COP is an indirect measure of postural sway and thus a measure of a persons ability to maintain balance.

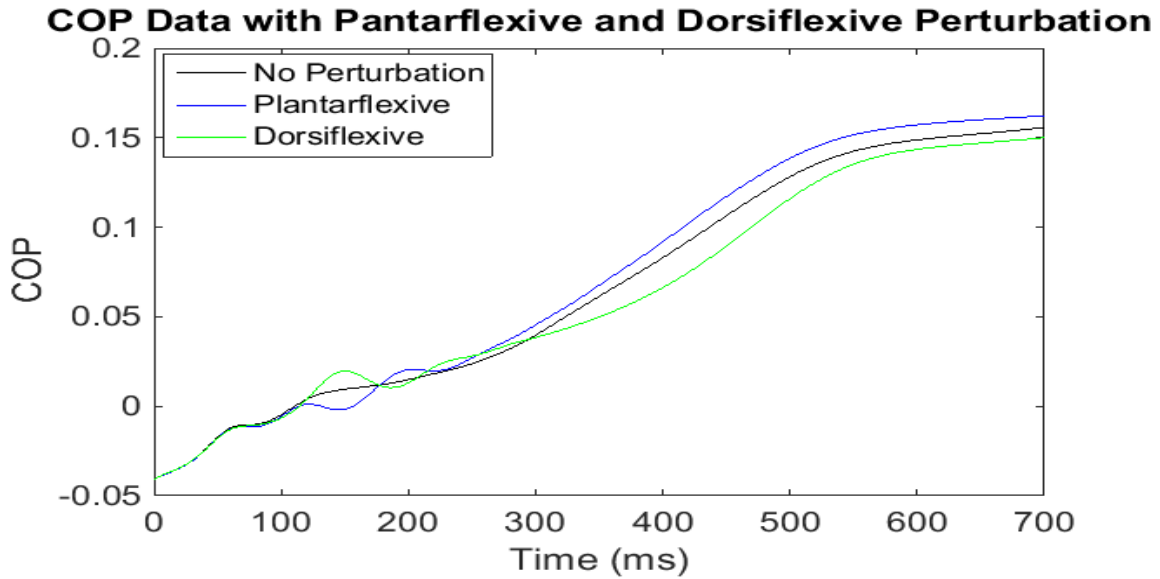


Figure 3.20: Center of pressure averaged over trials for subject AB118 with plantarflexive and dorsiflexive perturbations at 100 ms and 5°

3.7 COP Sine Fitting

On the graphs of the COP, such as in Figure 3.20, the oscillations that occur after the perturbations follow a sinusoidal form. Fitting the oscillations produce the following equation, as shown in Figure 3.21:

$$f(x) = a\sin(bx + c) + dx + f \quad (3.9)$$

where a is -0.004301, b is 0.09705, c is 6.132, d is 0.0002424 and f is -0.01318.

The black curve is the COP data at 100 ms plantarflexive perturbation at 5° from 100 ms to 225 ms, since the perturbation occurred at 100 ms point. The red curve is the sine fit to the perturbed data. The method used to fit the data to the sine curve in Figure 3.21 is nonlinear least squares with the LAR robust and the Levenberg–Marquardt algorithm. The starting point is at $(a, b, c, d, f) = (0.7606, 0.6114, 0.7901, 0.6797, 0.6551)$.

The goodness of fit for this sine curve fitting shows that $SSE=9.273e-06$, $R\text{-squared} = 0.9995$, and $RMSE = 0.000252$. This means that the fit is very well done and Equation (3.9) with the given values for the coefficients follows the perturbed COP data.

SSE is the Sum of Squares Due to Error. This statistic measures the total deviation of the response values from the fit to the response values. It is also called the summed square of residuals.

$$SSE = \sum_{i=1}^n w_i(y_i - \hat{y}_i)^2 \quad (3.10)$$

A value closer to 0 indicates that the model has a smaller random error component, and that the fit will be more useful for prediction.

The R-Squared statistic measures how successful the fit is in explaining the variation of the data. Put another way, R-square is the square of the correlation between the response values and the predicted response values. It is also called the square of the multiple correlation coefficient and the coefficient of multiple determination [10].

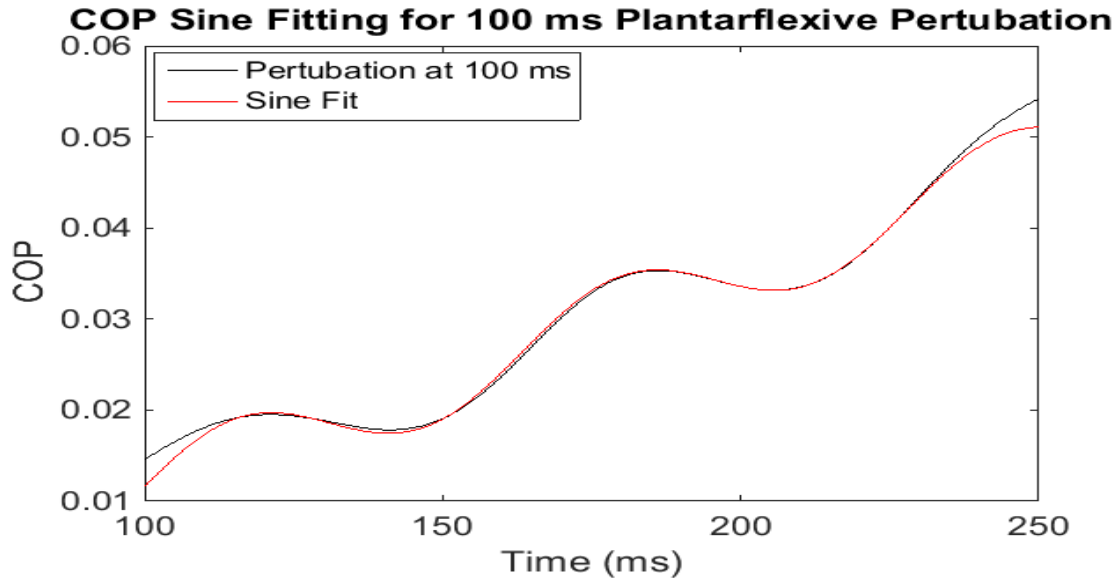


Figure 3.21: Sine fitting for center of pressure at 2° 100 ms plantarflexive perturbation for Subject AB 122.

R-square is defined as the ratio of the sum of squares of the regression (SSR) and the total sum of squares (SST). SSR is defined as

$$SSR = \sum_{i=1}^n w_i (\hat{y}_i - \bar{y})^2 \quad (3.11)$$

with w_i as the weighted variable and defined as

$$w_i = \frac{1}{Var(e_i)} \quad (3.12)$$

SST is also called the sum of squares about the mean, and is defined as

$$SST = \sum_{i=1}^n w_i (y_i - \bar{y})^2 \quad (3.13)$$

where $SST = SSR + SSE$. Given these definitions, R-square is expressed as

$$R - squared = \frac{SSR}{SST} = 1 - \frac{SSE}{SST} \quad (3.14)$$

R-square can take on any value between 0 and 1, with a value closer to 1 indicating that a greater proportion of variance is accounted for by the model. An R-square value of 0.9995 means that the fit explains 99.95% of the total variation in the data about the average [10].

3.8 Least Squares Analysis

After the ankle angle data was graphed in the time (ms) vs angle (θ) plots, it was logical to conduct the least squares model fitting. The best fit in the least-squares sense minimizes the sum of squared

residuals, a residual being the difference between an observed value and the fitted value provided by a model. Method of Least Squares is a procedure to determine the best fit line to data; the proof uses simple calculus and linear algebra. The basic problem is to find the best fit line [26]; for the example derivation, we assume y as

$$y = ax^2 + bx + c \quad (3.15)$$

for constants a, b, c , to be determined. The method easily generalizes to finding the best fit of the form

$$y = a_1 f_1(x) + .. + c_K f_K(x) \quad (3.16)$$

It is not necessary for the function f_k to be linear in x because all that is needed is that y is a linear combination of these functions. The method of the least squares [26] is described below.

Given data $(x_1, y_1), \dots, (x_i, y_i)$, we can define the error as

$$E(a, b, c) = \sum_{i=1}^N (y_i - (ax_i^2 + bx_i + c))^2 \quad (3.17)$$

with N being the number of data points. To avoid the problem with positive and negative residuals cancelling each other when summed, the sum of squared residuals is used as above. This is just N times the variance of the data set $y_1 - (a x_1^2 + b x_1 + c), \dots, y_i - (a x_i^2 + b x_i + c)$. The goal is to find values of a, b and c that minimize the error. The solution ensures that the sum of the errors from the mean function is as small as possible. This requires that the values of (a, b, c) satisfy

$$\frac{\partial E}{\partial a} = 0, \quad \frac{\partial E}{\partial b} = 0 \quad \text{and} \quad \frac{\partial E}{\partial c} = 0 \quad (3.18)$$

We can find the least squares curve by taking the partial derivatives of the sum of squares function with respect to the coefficients [26]. Differentiating $E(a, b, c)$ yields

$$\frac{\partial E}{\partial a} = \sum_{i=1}^N -2(y_i - (ax_i^2 + bx_i + c))(x_i^2) \quad (3.19)$$

$$\frac{\partial E}{\partial b} = \sum_{i=1}^N -2(y_i - (ax_i^2 + bx_i + c))(x_i) \quad (3.20)$$

$$\frac{\partial E}{\partial c} = \sum_{i=1}^N -2(y_i - (ax_i^2 + bx_i + c)) \quad (3.21)$$

A function has its minimum where the derivative is 0. After taking the derivative of E with respect to a , and with respect to b and also with respect to c , we need to set those three partial derivatives to 0. Setting $\frac{\partial E}{\partial a} = \frac{\partial E}{\partial b} = \frac{\partial E}{\partial c} = 0$, and then dividing by the common factor of -2 results in

$$0 = \sum_{i=1}^N (ax_i^4) + \sum_{i=1}^N (bx_i^3) + \sum_{i=1}^N (cx_i^2) + \sum_{i=1}^N (y_i x_i^2) \quad (3.22)$$

$$0 = \sum_{i=1}^N (ax_i^3) + \sum_{i=1}^N (bx_i^2) + \sum_{i=1}^N (cx_i) + \sum_{i=1}^N (y_i x_i) \quad (3.23)$$

$$0 = \sum_{i=1}^N (ax_i^2) + \sum_{i=1}^N (bx_i) + \sum_{i=1}^N (c) + \sum_{i=1}^N (y_i) \quad (3.24)$$

These equations can be rewritten as

$$\left(\sum_{i=1}^N (x_i^4) \right) a + \left(\sum_{i=1}^N (x_i^3) \right) b + \left(\sum_{i=1}^N (x_i^2) \right) c = \sum_{i=1}^N (x_i^2 y_i) \quad (3.25)$$

$$\left(\sum_{i=1}^N (x_i^2) \right) a + \left(\sum_{i=1}^N (x_i) \right) b + \left(\sum_{i=1}^N (1) \right) c = \sum_{i=1}^N (x_i y_i) \quad (3.26)$$

$$\left(\sum_{i=1}^N (x_i) \right) a + \left(\sum_{i=1}^N (1) \right) b + \left(\sum_{i=1}^N (1) \right) c = \sum_{i=1}^N (y_i) \quad (3.27)$$

The values of a and b which minimize the error are obtained and they satisfy the following linear system:

$$\begin{pmatrix} \sum_{i=1}^N (x_i^4) & \sum_{i=1}^N (x_i^3) & \sum_{i=1}^N (x_i^2) \\ \sum_{i=1}^N (x_i^3) & \sum_{i=1}^N (x_i^2) & \sum_{i=1}^N (x_i) \\ \sum_{i=1}^N (x_i^2) & \sum_{i=1}^N (x_i) & \sum_{i=1}^N (1) \end{pmatrix} \begin{pmatrix} a \\ b \\ c \end{pmatrix} = \begin{pmatrix} \sum_{i=1}^N (y_i x_i^2) \\ \sum_{i=1}^N (y_i x_i) \\ \sum_{i=1}^N (y_i) \end{pmatrix} \quad (3.28)$$

Solve for a , b , and c to get the coefficient values for $y = ax^2 + bx + c$. This was done in MATLAB. The data was fitted to the least squares method. The MATLAB code that was written is in Appendix A.

The following are Figures of ankle data with curve of fit using the described method above.

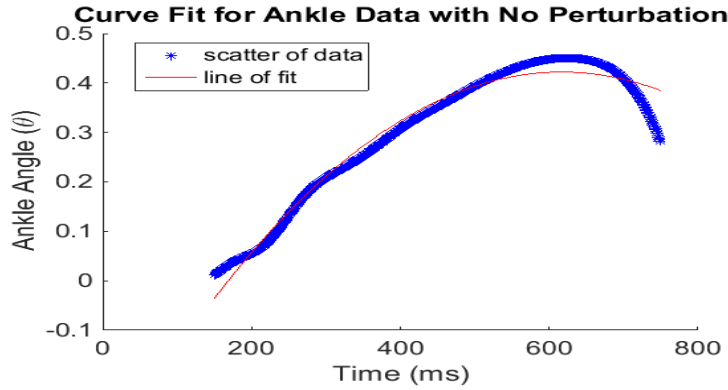


Figure 3.22: Curve fit using least squares method on the non perturbed ankle angle data of subject AB43.

As you can see from Fig. 3.22, the red line which is the parabola line of fit follows the trend of the data. This is the ankle angle with no perturbations. The MatLab code in Appendix A is used to generate Fig. 3.22 for subject AB43. The equation for the curve fit is

$$y_{fit} = -2.1053(10^6)x^2 + 0.002596x - 0.377843 \quad (3.29)$$

Fig. 3.23 presents the ankle angle data with the curve fit where the perturbation occurred at 100 ms at 2° . The equation of this curve of fit is

$$y_{fit} = -2.035043(10^6)x^2 + 0.0025823x - 1.979445 \quad (3.30)$$

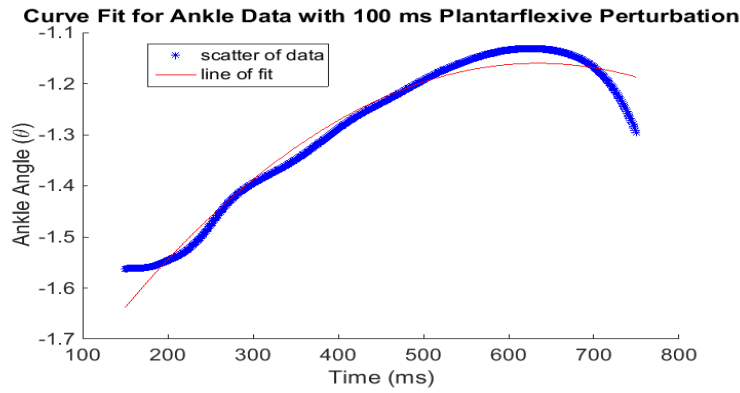


Figure 3.23: Curve fit for ankle data with 100 ms plantarflexive perturbation at 2° for subject AB43.

Fig. 3.24 shows the curve fit for ankle data with 225 ms perturbation at 2° . The perturbation occurs at 225 ms and the graph is from 275 ms to 750 ms to show the reaction after the occurrence of the perturbation on the ankle. The equation of this curve of fit is

$$y_{fit} = -2.4714438(10^6)x^2 + 0.0030806x - 2.11393597 \quad (3.31)$$

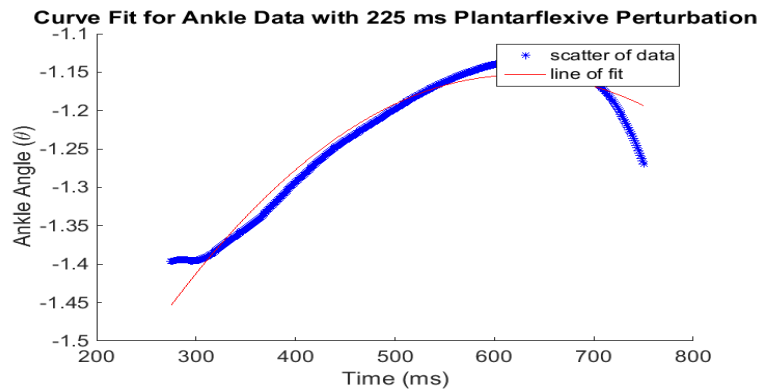


Figure 3.24: Curve fit for ankle data with 225 ms plantarflexive perturbation at 2° for subject AB43.

Fig. 3.25 shows the curve fit for ankle data with 350 ms perturbation at 2° . The perturbation occurs at 350 ms and the graph is from 400 ms to 750 ms to show the reaction after the occurrence of the perturbation on the ankle. The equation of this curve of fit is

$$y_{fit} = -4.831067(10^6)x^2 + 0.0059517x - 2.9446597 \quad (3.32)$$

The the curve fit equations for subject AB43 are similar. There is an increase in slope and a decrease in the y–intercept as the perturbation increases from non perturbation to 100 ms perturbation to 225 ms perturbation to 350 ms perturbation. The value of a decrease overall as the time point of perturbations increases. The value of b overall increases as the time point of perturbations increases, and the value of c decreases as the perturbations move. c shows the biggest change in value, where as other variables slightly changed in value.

As for patient to patient, the same trend follows but the initial non–perturbtd curve is unique to each patient. Then as each perturbation occurs for each patient, the values of a , b , and c behave very

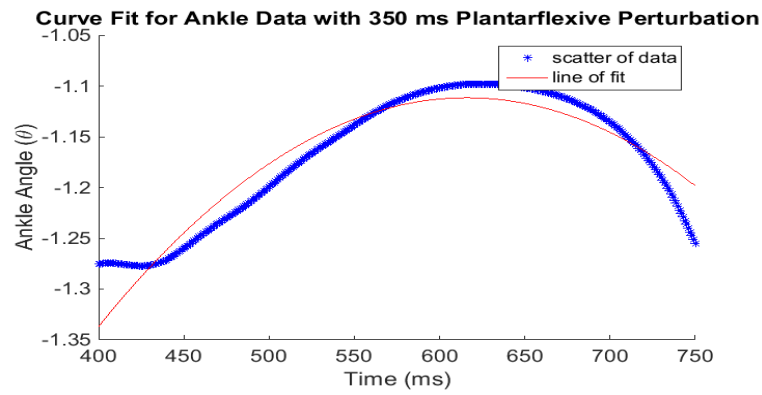


Figure 3.25: Curve fit for ankle data with 350 ms plantarflexive perturbation at 2° for subject AB43.

similarly, even though there is patient to patient variability. After looking at the curve fit equations that were conducted on the data of different patients, there is a definite trend in how the curves change due to the different perturbations.

Chapter 4

Conclusion

4.1 Conclusion

This study used various methods to analyze and describe the data gathered from the stance phase of the gait cycle. This gives more insight as to how the perturbations affect the walk cycle. Ankle characteristics vary in terms of gait phase and perturbation changes. It can be mimicked with uneven ground, surface with rocks on it or small potholes in the ground.

After calculating the minimums and maximum for the ankle angle, the total range of motion is calculated by taking the absolute values of the global minimum and maximum and adding the two values. This is beneficial in using this ROM for biomechanical uses. Knowing how the foot reacts with respect to the perturbations is important in several real life applications. It helps to better understand the stability in people's gait. It can further expand research in biomathematics and coincide with similar gait studies. The COP relates to the balance of the foot, which results in better stability. It is dependent on the position of the body with respect to the supporting surface. The shifts of the COP data indirectly portrays postural sway and thus a measure of a person's ability to maintain balance. And increase in the sway from the minimal sway that occurs from standing has some indication of poorer balance as well as a decrease neuromuscular control.

This study is useful for designing better shoes. For example, Nike Air running shoes which have substantial cushioning under the heel can be improved to reduce injury even more. The center of pressure can indicate changes to the design of the insole of the shoe. Looking at how typically perturbed COP returns to its pattern of no perturbation can be significant for Nike. The article by Lohman further discusses the effects of minimalist shoes on running gait in terms with a focus on center of pressure and ground reaction force analysis [24]. Another application is orthopaedic devices. These findings may be clinically applicable in the design and development of ankle prosthetic devices that can naturally replicate human walking on uneven surface. By analysing the human gait cycle with emphasis on the observations of how the ankle moves and the range of motion, it will contribute to making better orthopaedic devices such as prosthetics. In addition to the articles mentioned in Section 3.1, the article "The Human Ankle During Walking: Implications for Design of Biomimetic Ankle Prostheses" by Andrew Hansen [19] relates to the study of gait. It talks about using the ankle angle of the foot along with the moment to examine the quasi-stiffness of the ankle to use in the design of ankle prostheses. These articles depict only a portion of such vast research. Exploring the characteristics of

gait will bring greater insight into providing solutions to better prosthetics.

4.2 Suggestions for Changes

After conducting this study, there are several points to consider. The subjects that were used had different demographics that were not listed in the data. Also, measurement errors must always be taken into account when different measurements are taken. It is human error and could have some impact on the calculations.

A suggestion for further research would be to conduct or find a similar study with descriptions of the subjects, such as testing all females and then all males, testing based on age brackets, and height and weight categories. These more detailed results of each demographic may show more insight into each group and the pattern on gait that it has. Also, studying posture in addition to the gait will aid in analyzing the balance of the subjects.

In addition, conducting this experiment and analysing the data that includes running patients as well as walking patients will allow to compare the two different gaits of walking and running. These articles “Motor Patterns in Human Walking and Running” by Cappellini [6] and “Differences in Muscle Function During Walking and Running at the Same Speed” by Sasaki [34] discuss the difference of the gaits of walking and running. This will further allow better calculations for orthopaedic shoes and devices.

Appendix A

MATLAB Code

Least Squares code to determine coefficients a , b , c when the function is $y = ax^2 + bx + c$.

Main file

```
1 close all; clc; clear all;
3
4 format long
5 cd ..
6 cd '2 deg study'
7
8 load AB43_Data.mat;
9
10 A=Foot_Shank_Ang.HCref;
11
12 xdata = [200:1:800];
13
14 L=length(xdata);
15
16 for i=1:850
17     AverageA(i)=mean(A(i,:));
18     StdDevA(i)=std(A(i,:));
19 end
20
21 ydata=AverageA(:,200:800);
22
23 A = zeros(3,3);
24 R = zeros(3,1);
25
26 for j=1:3
27     A(1,j)=2*sum(xdata.^(5-j));
28     A(2,j)=2*sum(xdata.^(4-j));
29     A(3,j)=2*sum(xdata.^(3-j));
30
31 end
32
33 for i=1:3
34     R(i,1)=2*sum(ydata.*xdata.^(3-i));
35
```

```

end
37
C=A\R;
39 time=[200:1:800];

41 figure(1)
scatter(time,ydata,'b','*')
43 hold on
yfit=C(1)*xdata.^2+C(2)*xdata+C(3);
45
plot(time,yfit,'-r')
47
title('Curve Fit')
49 xlabel('Time (ms)')
ylabel('Ankle Angle (\theta)')
51 legend('scatter of data', 'line of fit')

53 set(gcf,'Color','white')
set(0,'defaultaxesfontsize',16)

```

Bibliography

- [1] S.K. Au and H.M. Herr. *Powered Ankle-Foot Prosthesis*, 2008 (accessed 2015-2-27). http://biomech.media.mit.edu/wp-content/uploads/sites/3/2013/07/Au_Herr_Magazine_200.pdf.
- [2] A.S. Batuev and O.P. Tairov. *Hill's Equation of Muscle Contraction*, 2010 (accessed 2015-1-28). <http://encyclopedia2.thefreedictionary.com/Hill%27s+Equation+of+Muscle+Contraction>.
- [3] B.J. Benda, P.O. Riley, and D.E. Krebs. Biomechanical relationship between center of gravity and center of pressure during standing. *IEEE Transactions on Rehabilitation Engineering*, 2:3–10, 1994.
- [4] Boundless. *Types of Muscle Contractions: Isotonic and Isometric*, 2015 (accessed 2015-1-28). <https://www.example.com/physiology/textbooks/boundless-anatomy-and-physiology-textbook/muscle-tissue-9/control-of-muscle-tension-97/types-of-muscle-contractions-isotonic-and-isometric-546-84>
- [5] J. W. Brodsky, F.E. Polo, S.C. Coleman, and N. Bruck. Changes in gait following the Scandinavian total ankle replacement. *Journal of Bone and Joint Surgery*, 93:1890–1896, 2011.
- [6] G. Cappellini, Y.P. Ivanenko, R.E. Poppele, and F. Lacquaniti. *Motor Patterns in Human Walking and Running*, 2006 (accessed 2015-3-15). <http://jn.physiology.org/content/95/6/3426>.
- [7] J.A. DeLisa and B.M. Gans. *Physical Medicine and Rehabilitation: Principles and Practice*. Lippincott Williams and Wilkins, 2010.
- [8] MathWorks: Documentation. *One-sample Kolmogorov–Smirnov test: kstest*, 2015 (accessed 2015-2-14). <http://www.mathworks.com/help/stats/kstest.html?searchHighlight=kstest>.
- [9] MathWorks: Documentation. *One-sample and paired-sample t-test: ttest*, 2015 (accessed 2015-2-16). <http://www.mathworks.com/help/stats/ttest.html>.
- [10] MathWorks: Documentation. *Evaluating Goodness of Fit*, 2015 (accessed 2015-2-19). <http://www.mathworks.com/help/curvefit/evaluating-goodness-of-fit.html>.
- [11] MathWorks: Documentation. *Histogram with a distribution fit: histfit*, 2015 (accessed 2015-2-21). <http://www.mathworks.com/help/stats/histfit.html?searchHighlight=histfit>.
- [12] MathWorks: Documentation. *Correlation Coefficients: corrcoef*, 2015 (accessed 2015-2-24). <http://www.mathworks.com/help/matlab/ref/corrcoef.html>.

- [13] MathWorks: Documentation. *Covariance: cov*, 2015 (accessed 2015-2-25). <http://www.mathworks.com/help/matlab/ref/cov.html?searchHighlight=cov>.
- [14] F. Farahmand, T. Rezaeian, R. Narimani, and P. Hejazi Dinan. *Kinematic and Dynamic Analysis of the Gait Cycle of Above-Knee Amputees*, 2006 (accessed 2015-2-25). Sharif University of Technology.
- [15] B. Furman and K. Youssefi. *Structures and Stiffness*, 2007 (accessed on 1014-10-16). http://www.engr.sjsu.edu/bjfurman/courses/E10/E10pdf/Structures_Stiffness.pdf.
- [16] R. D. Gregg, E. J. Rouse, L. J. Hargrove, and J. W. Sensinger. Evidence for a time-invariant phase variable in human ankle control. *PLoS One*, 9:e89163:1–13, 2014.
- [17] R. D. Gregg, E. J. Rouse, L. J. Hargrove, and J. W. Sensinger. *Data from: Evidence for a time-invariant phase variable in human ankle control*, *Dryad Digital Repository*, 2015 (accessed 2014-10-8). <http://datadryad.org/resource/doi:10.5061/dryad.rm505>.
- [18] Analyse-It: User Guide. *Passing Bablok Regression*, 2015 (accessed 2015-3-1). http://analyse-it.com/docs/220/method_evaluation/passing_bablok_regression.htm.
- [19] A.H. Hansen, D.S. Childress, S.C. Miff, and S.A. Gard. *The Human Ankle During Walking: Implications for Design of Biomimetic Ankle Prostheses*, 2004 (accessed 2015-3-12).
- [20] E. Howard. *Topic 15: Muscle Mechanics*, 2014. http://www.google.com/url?sa=t&rct=j&q=&esrc=s&source=web&cd=1&ved=0CB4QFjAA&url=http%3A%2F%2Fcmrg.ucsd.edu%2FCourses%2Fbe112a%2FTopics%3Faction%3DAttachFile%26do%3Dget%26target%3Dbe112aTopic16_MuscleMechanics_EHowardVersion.ppt&ei=xJ7rVJP2A6SSsQTwg4KADA&usg=AFQjCNGyQ2wxwtUrFVS0o34sXvt8IcTUw&sig2=Am8skLJJd9ihE_usgYPnyg&bvm=bv.86475890,d.cWc.
- [21] B. Johnson. *Small Muscles...Big Gains*, 2011 (accessed 2015-2-1). <http://runningdownadream23.com/tag/weight-loss/>.
- [22] P. R. Khuman. *Gait: Normal and Abnormal from M.P.T., Ortho and Sports*, 2012. <http://www.slideshare.net/prkhuman/gait-normal-abnormal>.
- [23] D. Lafond, M. Duarte, and F. Prince. Comparison of three methods to estimate the center of mass during balance assessment. *Journal of Biomechanics*, 37:1421–1426, 2003.
- [24] E.B. Lohman. *Effects of Minimalist Shoes on Running Gait*, 2002 (accessed 2015-3-3). <http://www.georgiagamechangers.com/index.php/in-the-news/21-minimalist-shoes>.
- [25] J. L. McNitt-Gray. *Angular Kinematics Lab*, 2014. <http://dornsife.usc.edu/labs/biomech/publications>.
- [26] S. J. Miller. *The Method of Least Squares*, *Brown University*, 2007 (accessed on 1015-2-3). http://web.williams.edu/Mathematics/sjmiller/public_html/BrownClasses/54/handouts/MethodLeastSquares.pdf.
- [27] A. H. Mohammed. *The Gait Cycle*, 2014. <http://www.sciencedirect.com/science/article/pii/S1110863015000026>.

- [28] C.S. Moriguchi, T.O. Sato, and H.J.C. Gil Coury. Ankle movement during normal gait evaluated by flexible electrogoniometer. *Brazilian Journal of Physical Therapy*, 11:205–211, 2007. University of Sao Carlos.
- [29] C.S. Moriguchi, T.O. Sato, and H.J.C. Gil Coury. *Ankle Movements During Normal Gait Evaluated By Flexible Electrogoniometer*, 2007 (accessed 2015-2-19). <http://www.scielo.br/pdf/rbfis/v11n3/a06v11n3>.
- [30] C. Oatis. *Kinesiology: The Mechanics and Pathomechanics of Human Movement*. Lippincott Williams and Wilkins, 2007.
- [31] J. Petrucci, B. Nandram, and M. Chen. *Applied Statistics for Engineers and Scientists*. Pearson, 1999.
- [32] S Robinovitch. *Muscle Mechanics*, 2006. http://www.sfu.ca/~steve/kin840/lecture_outlines/lecture_4_muscle.pdf.
- [33] M. Sarmini. *Understanding Normal and Pathological Gait*. http://www.google.com/url?sa=t&rct=j&q=&esrc=s&source=web&cd=1&ved=0CB4QFjAA&url=http%3A%2F%2Fwww.medschool.lsuhsu.edu%2Fphysical_medicine%2FPPT%2FNormal_Pathological_Gait.ppt&ei=pCbtVIPLFMznsASR2YKQAQ&usg=AFQjCNGuVEZzmDqCfqj9Apq1KuxqwGRn5w&sig2=qWq5pVYYGn5y9KUBWj44UQ&bvm=bv.86475890,d.cWc.
- [34] K. Sasaki and R.R. Neptune. *Differences in Muscle Function During Walking and Running at the Same Speed*, 2005 (accessed 2015-3-15). <http://www.me.utexas.edu/~neptune/Papers/job39%2811%29.pdf>.
- [35] R.J. Seidman. *Structure and Function of Skeletal Muscle*, 2012 (accessed 2014-10-01). <http://courses.washington.edu/conj/motor/musclereview.htm>.
- [36] R.J. Seidman. *Skeletal Muscle Structure*, 2014 (accessed 2014-10-05). <http://emedicine.medscape.com/article/1923188-overview#>.
- [37] R. Shadmehr and S. P. Wise. *A Simple Muscle Model*, 2015 (accessed on 1014-11-21). <http://www.shadmehrlab.org/book/musclemodel.pdf>.
- [38] D. Thelen and C. Decker. *Biomechanics: Foot Force Measured by a Force Platform*, 2009. <http://silver.neep.wisc.edu/~lakes/BME315L2a.pdf>.
- [39] M. L. Thies. *Introduction to the Skeletal System*, 2014 (accessed 2014-11-18). http://www.shsu.edu/~bio_mlt/Chapter7.html.
- [40] D. Thompson. *Ground Reaction Force*, 2002 (accessed 2014-11-27). <http://moon.ouhsc.edu/dthompsogait/kinetics/GRFBKGN.DHTML>.
- [41] E.W. Weisstein. *Kolmogorov Smirnov Test*, 2015 (accessed 2015-2-6). <http://mathworld.wolfram.com/Kolmogorov-SmirnovTest.html>.
- [42] C. Yau. *R Tutorial: Correlation Coefficient*, 2015 (accessed 2015-1-15). <http://www.r-tutor.com/elementary-statistics/numerical-measures/correlation-coefficient>.